
CARBONATE ROCKS
OF THE
KIRKLAND LAKE-LARDER LAKE GOLD CAMP

THE MINERALOGICAL COMPOSITION
OF THE
CARBONATE ROCKS
OF THE
KIRKLAND LAKE-LARDER LAKE GOLD CAMP

BY

SHARON LOUISE TIHOR, B.Sc.
(née PHILLIPS).

A Thesis

Submitted to the School of Graduate Studies

in Partial Fulfilment of the Requirements

for the Degree

Master of Science

McMaster University

May 1978

MASTER OF SCIENCE (1978)
(Geology)

McMASTER UNIVERSITY
Hamilton, Ontario

TITLE The Mineralogical Composition of the Carbonate Rocks of the
Kirkland lake-Larder Lake Gold Camp

AUTHOR Sharon Louise Phillips B.Sc. University of Calgary
Sharon Louise Tihor B.Sc. Lakehead University

SUPERVISORS Dr. J. H. Crocket
Dr. H. D. Grundy

NUMBER OF PAGES viii, 93

ABSTRACT

The quartz-carbonate horizon of the Kirkland Lake-Larder Lake area of Ontario is the subject of continuing controversy over its origin, and relationship with the surrounding rocks and the many gold occurrences.

Part of the essential information required is the carbonate mineralogy of the rocks. In the past the carbonate minerals have been identified by optical and presumably chemical means.

In the present study the carbonate mineralogy was determined using X-ray diffraction and scanning electron microscopic techniques. To the author's knowledge, this is the first time these techniques have been employed in an analysis of the quartz-carbonate rocks of the Kirkland Lake-Larder Lake area.

The quartz-carbonate rocks consist mainly of quartz, magnesite, dolomite, chlorite, albite and muscovite with accessory amounts of pyrite, rutile, talc and possibly leucoxene and ankerite.

A semi-quantitative estimate of the percentages of quartz, dolomite and magnesite was made using X-ray diffraction, and two series of prepared standards.

The possibility of a correlation between the carbonate mineralogy and known gold deposits was also explored. The data obtained in this study tend to tentatively suggest a positive correlation between magnesite in the quartz-carbonate rocks and the known gold deposits.

AKNOWLEDGEMENTS

Dr. J. D. Crocket and Dr. H. D. Grundy of McMaster University jointly supervised the process and completion of this thesis. I thank them for their assistance, interest and guidance. Financial assistance was provided by the National Research Council of Canada.

My thanks are extended to Mr. L. A. Tihor who provided many rock samples, the chemical analyses and useful discussion.

I wish to extend special thanks to my friend and colleague Dr. R. A. Jones, who cajoled, advised, assisted and threatened at appropriate times and made it easier to finish a difficult task.

Thank you also to my parents for their support and to my daughter Karen for being Karen.

TABLE OF CONTENTS

Abstract	iii
Aknowledgements	iv
Table of Contents	v
List of Illustrations	
Figures	vii
Plates	vii
List of Tables	viii
List of Maps	viii

Chapter One Background

1.1 Introduction	1
1.2 Geological Setting	
1.2.1 General Geology	2
1.2.2 Gold Mineralization	4
1.3 Previous Work Concerning the Carbonate Zones --- With Commentary	4.

Chapter Two Field and Laboratory Methods

2.1 Sample Collection and Preparation	9
2.2 Whole Rock Analysis by X-ray Diffraction	9
2.3 Quantitative Analysis of the Carbonate Minerals by X-ray Diffraction	
2.3.1 Introduction	13
2.3.2 Standards- Preparation and Analysis	13

2.3.2.1 ST-1 to ST-9 Magnesite plus Dolomite	13
2.3.2.2 ST-1 to ST-9 Magnesite plus Quartz	20
2.3.3 Semiquantitative Analysis of Powdered Rock Samples	23
2.3.4 Interference with the Major Carbonate Peaks by the Quartz Peaks	24
2.4 Thin Sections	25
2.4.1 Transmitted Light Microscopy	25
2.4.2 Scanning Electron Microscopy (SEM)	26
2.5 Mineral Staining	27
 Chapter Three Results and Observations	
3.1 Whole Rock Powder Scans	30
3.2 Semiquantitative Analysis of Powdered Rock Samples	30
3.3 Thin Sections - Transmitted Light Microscopy	43
3.4 Thin Sections - Scanning Electron Microscopy	53
 Chapter Four Discussion and Conclusions	81
 Appendices	88
 Bibliography	92

LIST OF ILLUSTRATIONS

Figures

- 2.1 Position and Intensity of the Diagnostic Beaks of the Major Rock Forming Minerals
- 2.2 1st, 2nd and 3rd Powder Runs of ST-1 to ST-9
- 2.3 1st Powder Run of ST-21 to ST-29
- 2.4 Staining Schedule for Carbonates
- 3.1 Percentage of Magnesite and Dolomite
- 3.2 Percentage of Quartz and Magnesite
- 3.3 Percentage of Quartz, Magnesite and Dolomite

Plates

- 3.1 Quartz vein
- 3.2 Massive green quartz-carbonate
- 3.3 Pyrite grain in mica band
- 3.4 Twinning patterns in vein carbonates
- 3.5 Strain patterns in polycrystalline quartz grains
- 3.6 Twinning and recrystallization patterns in vein carbonates
- 3.7 A-H EB-2 Area 1
- 3.8 A-D EB-2 Area 2
- 3.9 A-E MG-11 Area 1
- 3.10 A-D MG-11 Area 2

Plates (cont.)

- 3.11 A-E MV-2
- 3.12 A-G EB-2 Area 3
- 3.13 A-H EB-2 Area 4

LIST OF TABLES

- 2.1 First Powder Run of ST-1 to ST-9
- 2.2 Second Powder Run of ST-1 to ST-9
- 2.3 Third Powder Run of ST-1 to ST-9
- 2.4 First Powder Run of ST-21 to ST-29
- 3.1 Whole Rock Scans from 5° to 60° of Two Theta
- 3.2 Semiquantitative Analysis of Powdered Rock Samples
- 3.3 Approximate Mineral Percentages
- 3.4 Summary of the Subject and Interpretation of Plates
3.7 to 3.13

LIST OF MAPS

- Map 1 Location map
- Map 2 Study area with sample locations

Chapter One Background

1.1 Introduction

The Kirkland Lake-Larder Lake Gold Camp is an area that has experienced continuous mining activity since the late 1800's. There are a large number of past producers of gold in the camp, as well as the Kerr-Addison and Maccasa mines which are presently mining gold.

The free gold occurs generally in quartz veins associated with two main rock types. In the north central part of the camp the gold deposits are associated with syenitic rock, and in the eastern sector with carbonate rocks, particularly the green quartz-carbonate. The latter association occurs in the Kerr-Addison mine.

The present author believes that a misleading picture of the carbonate mineralogy in the Kirkland Lake-Larder Lake Gold Camp has arisen, through no particular fault of the earlier investigators. Therefore the primary purpose of this study was to determine the mineralogy, particularly the carbonate mineralogy of the quartz-carbonate horizon along the full strike length of the camp. X-ray diffraction was used to identify the carbonate minerals and to the author's knowledge, this was the first X-ray diffraction study of these carbonates.

The second purpose of the study was to determine whether or not a correlation between the character of the carbonate mineralogy

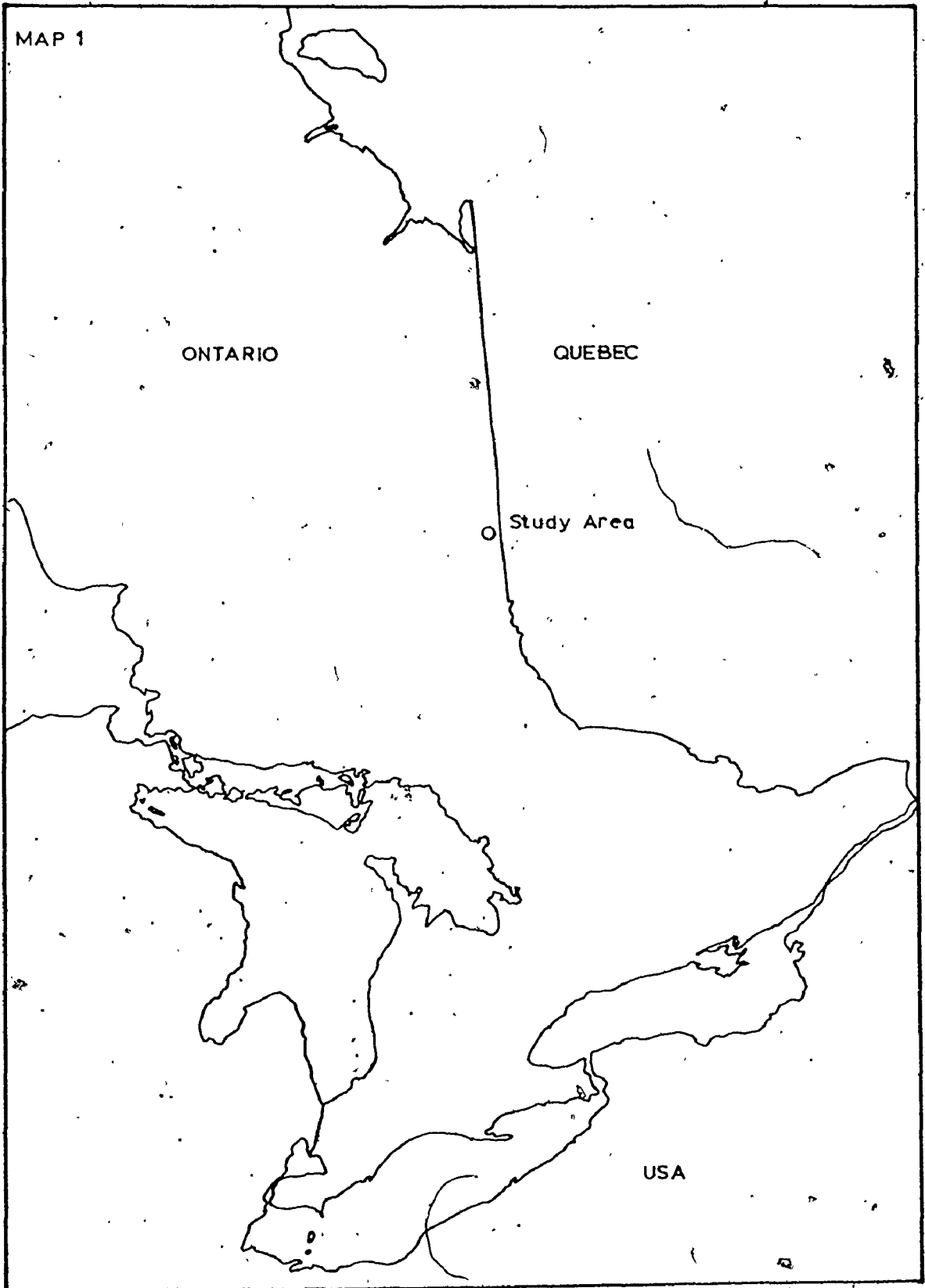
and the distribution of the known gold deposits could be established.

1.2 Geological Setting

1.2.1 General Geology

The general geology of the Kirkland Lake-Larder Lake area has been the subject of a number of studies in the past including Thompson(1941-1948), Goodwin(1965), Ridler(1969), and Hyde(1977). These studies have established that the geology is dominated by a large domical volcanic complex several miles in diameter. The rocks are Archean in age and form part of the world famous Abitibi Greenstone Belt(see Map 1). The base of the dome consists of thick mafic volcanic flows overlain by intermediate volcanic flows and breccias. These units are capped by felsic pyroclastics and clastic sediments. The general stratigraphy is similar to that observed at the many other large volcanic complexes common to the Abitibi Greenstone Belt. Concentrations of various metals are commonly associated with the upper stratified zones of the volcanic complexes, and in the Kirkland Lake-Larder Lake area the economically viable metals are gold and silver(Goodwin, 1965).

The structure of the area is complex and is generally accepted to be a doubly plunging complex anticline in the Kirkland Lake area, and a doubly plunging syncline in the Larder Lake area. According to Goodwin(1965) the Kirkland Lake complex is situated on the northeast flank of a larger regional anticline. The trend of the structure is persistently east-west. Further Goodwin(1965) states that the Larder Lake Break(see Map 2), a steeply dipping major fault



zone, is present across the area, and parallels the regional structure.

1.2.2 Gold Mineralization

The gold mineralization in deposits in the quartz-carbonate occurs almost exclusively as free gold in the Kirkland Lake-Larder Lake area. A regional control on the gold mineralization is the occurrence of gold-bearing quartz-carbonate veins in, or adjacent to, structural features which are part of the well-known Larder Lake Break. The Larder Lake Break is found on the southern edge of, or within the Timiskaming Group (see Map 2).

In the northern part of the Kirkland Lake area, particularly in Lebel and Teck townships, the gold occurs in a myriad of quartz veins in syenites and sediments; as well as along, or adjacent to the structural breaks. In the Larder Lake area the gold mineralization occurs in quartz stockworks in carbonate zones. These carbonate zones are generally strongly sheared, and are in, or adjacent to, the forementioned Larder Lake Break. In this latter region, the carbonate zones are hosted by a variety of rocks including basalts, dacites, syenites, tuffs and talc chlorite schists (Goddwin, 1965).

Both the stratigraphic position of the carbonate zones and the wide variety of rocks which compose the hosts have led to considerable controversy over the nature and origin of these zones.

1.3 Previous Work Concerning the Carbonate Zones --- with Commentary

The carbonate zones are generally referred to as the green quartz-carbonate rocks. This terminology is largely due to the fact

that carbonated rocks are often pervaded by a stockwork of white quartz veins and the carbonate portions are bright green. This feature is best shown in the Larder Lake area where carbonated rocks are abundant and where they host the major portion of the Kerr-Addison ore bodies. The green colour results from the presence of the chrome-bearing muscovite ---fuchsite.

Not all carbonate rocks however, have the above described appearance. The volume of quartz veins can vary considerably and the colour of the carbonate ranges from green to grey to light brown or buff. The peculiar appearance and stratigraphic position of the carbonate horizon has attracted comment and speculation since its presence was first noted. In the review of previous studies which follows below, note is made of the basis on which carbonate mineralogy has been assessed.

R. W. Brock(1907) initially describes the carbonates as "rusty weathering dolomite?", and as "dolomite" in the remainder of his report(Brock's quotation and question marks). He reports that the quartz-carbonate rock contains 60 percent lime-magnesia-iron carbonate with the remainder of the rock consisting of quartz and a soft green talcose silicate, probably serpentine. With regard to the carbonate zones, Brock reports that the carbonate horizon is conformable with the surrounding rocks, and is therefore an altered stratified ferrous dolomite, i.e. a member of the iron formation. The method used in determining the identity of the carbonates is not mentioned.

H. C. Cook(1922) conducted an extensive petrographic study

using thin sections and his report includes detailed descriptions of what he considers to be alteration zones of the country rock to carbonates. He identifies the carbonates as ankerite or a mixed carbonate of lime, iron and magnesia. He identifies calcite as the mineral occupying the oldest veins and refers to the whole alteration process as dolomitization. He also notes the presence of albite. Unfortunately, at no time does he state the criteria used in identifying the carbonate minerals. There is no reference to XRD or chemical analyses in Cook's paper and presumably mineralogical identifications are based on thin section optics.

G. W. Bain(1933) in a paper concerning the wall rock mineralization in Ontario gold deposits, considers the carbonate to be a result of carbonitization. He refers to the carbonate as simply "carbonate" and makes no mention of specific minerals.

C. P. Jenny(1941) in a report on the Omega Mine refers to the carbonates as carbonate rock or "dolomite"(Jenny's quotation marks) and describes them as calcium, magnesium and iron carbonates. He suggests that the carbonates are of secondary origin and are due to the replacement of country rock by magmatic solutions high in carbonate. Again there is no mention of the methods and criteria used to identify the elements and minerals.

D. W. Tully(1963), in a paper on the Upper Canada Mine, reports that he recognized dolomite, calcite, and ankerite in the alteration zones. He considers the alteration to be due to carbonitization and sericitization. He does not state his methods or criteria for identifying the carbonate minerals.

J. Mehar and C. Doning(1966), in a mine handout sheet describing the geology of the Kerr-Addison Mine, refer to the carbonate zones as carbonate or dolomite and consider that the carbonate zones are due to carbonitization.

R. H. Ridler(1969) in a study concerning the relationship of mineralization to volcanic stratigraphy in the Kirkland Lake area states that, "...judging by colour, all varieties from ankerite to limestone are present". In a later publication (1970) Ridler refers to the carbonate rocks without reference to specific carbonate mineralogy and considers the unit to be the carbonate facies of the Boston Iron Formation and exhalative in origin.

There are only two published analyses of the carbonate rocks. These chemical analyses are reported in Thompson(1941) and in the Kerr-Addison mine handout sheet, and indicate values of 4.17% to 19.69% CaO, 5.59% to 8.37% FeO, and 15.54% to 21.08% MgO. The present author is not aware of any previously published X-ray diffraction analyses. The earlier workers began referring to the carbonate minerals, with varying degrees of confidence, as dolomite (most often) or ankerite (occasionally), or as just carbonate. Later workers appear to have assumed that the carbonates were dolomite or ankerite, ignoring the reservations, in the form of quotation and question marks, of the earlier authors.

Presumably, most of the above mentioned identifications are based on optical mineralogy, but the problems associated with this method become readily apparent after one actually examines thin sections of the carbonate rocks.

Part of the fundamental information required to resolve this controversy is a determination of the actual identity of the carbonate minerals, and their distribution across the Kirkland Lake-Larder Lake Gold Camp. As has been previously stated (see Introduction) the acquisition of the above information, by field and laboratory techniques formed the basic purpose of this thesis. Details of this research project are outlined in the text following and the results of the investigation are described herein.

Chapter Two Field and Laboratory Methods

2.1 Sample Collection and Preparation

Samples of the quartz-carbonate horizon utilized in the study were collected by the author during two visits to the field area in the summers of 1974 and 1975. A large number of additional samples in powder form were made available by L. A. Tihor and were collected during the summers of 1974, 1975 and 1976. The sample sites cover the exposed length of the carbonate horizon in the Kirkland Lake-Larder Lake camp as shown on Map 2.

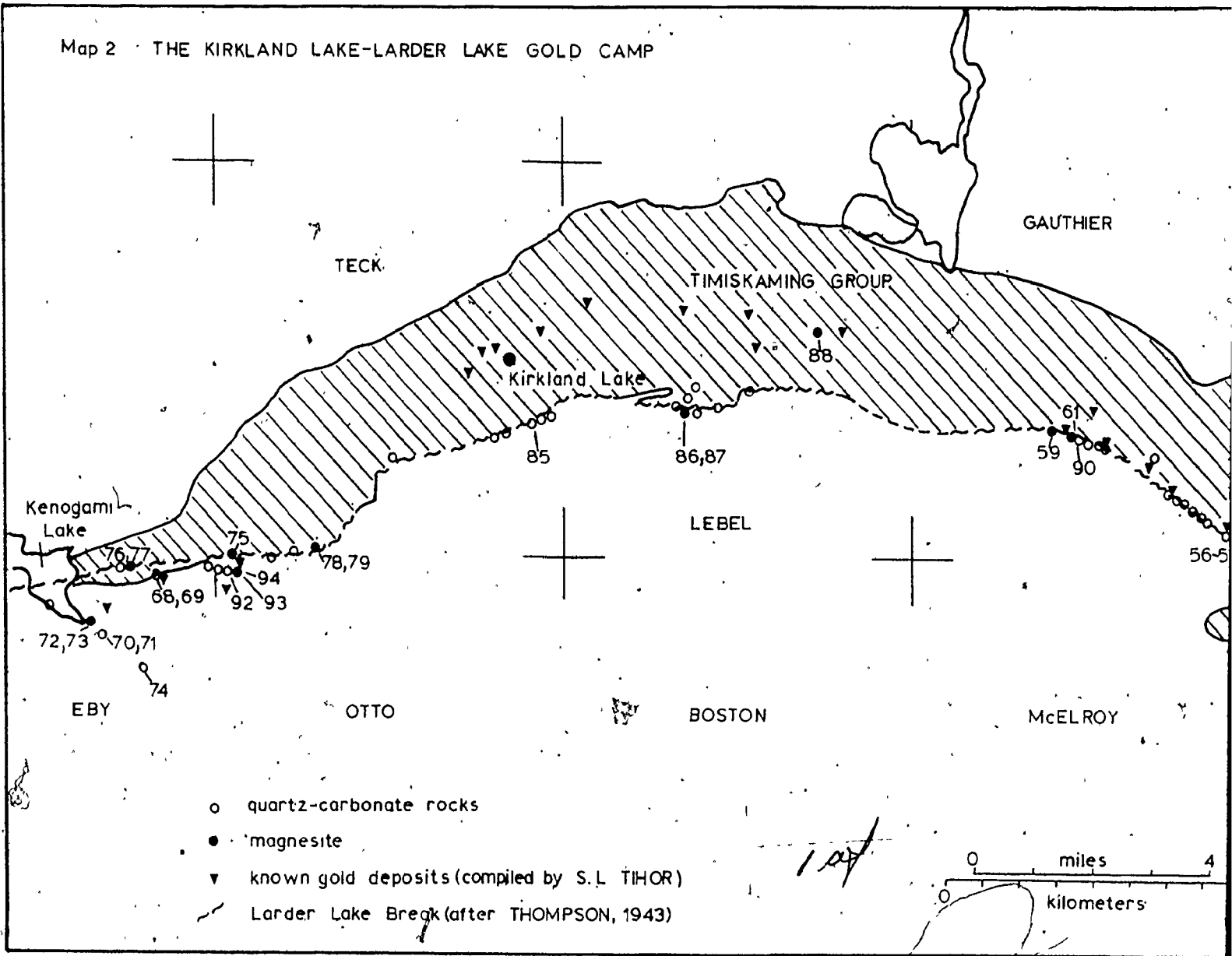
A representative portion of each sample was powdered using firstly a jaw crusher, followed by a disc pulverizer and finally a shatter box. The resulting -200 mesh powders were then stored in glass vials.

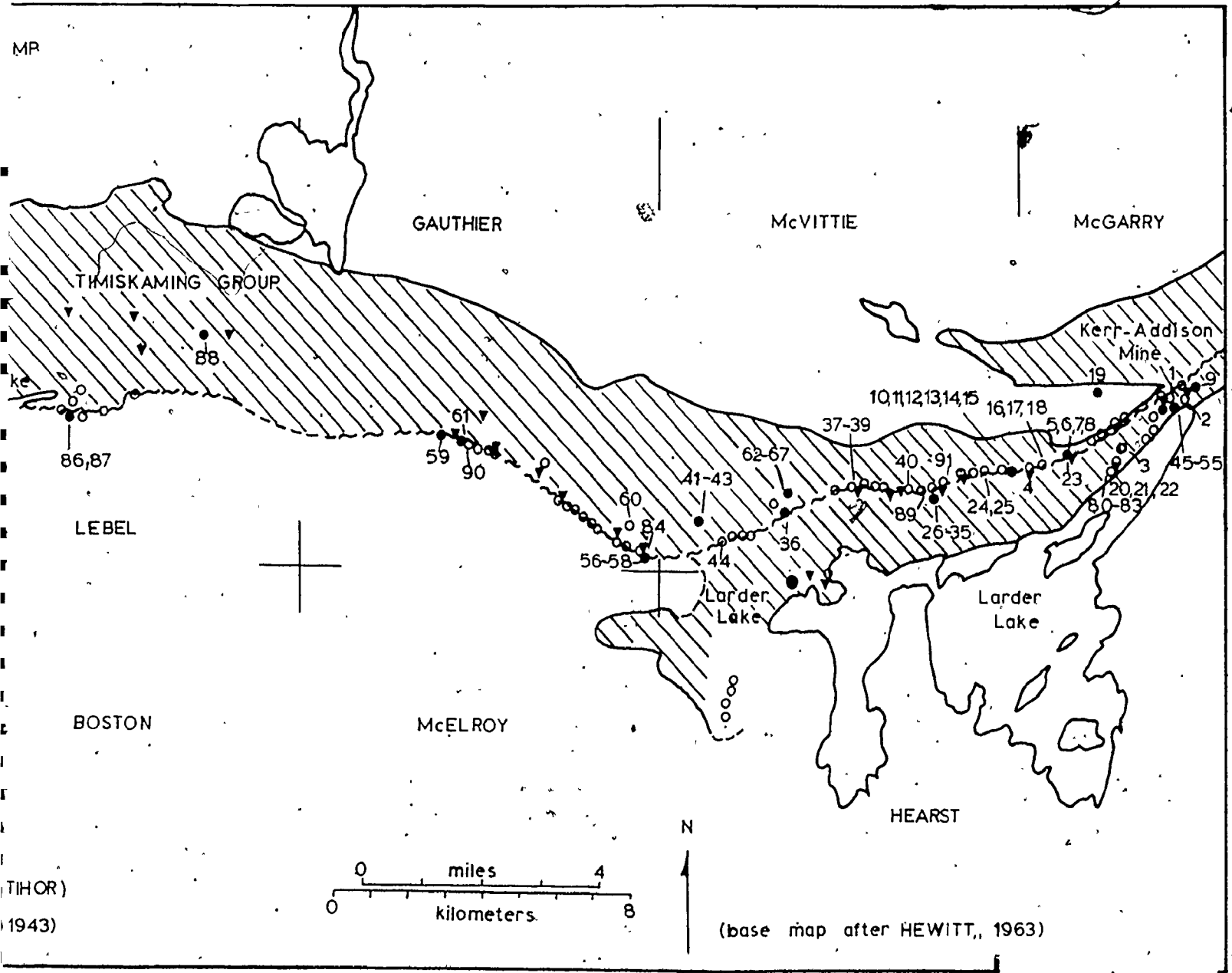
2.2 Whole Rock Analysis by X-ray Diffraction

X-ray diffraction was the most powerful survey method for determining the carbonate minerals present in the rock powders. Thin sections were also used in identifying the other minerals present.

In the initial phase of this series of analyses, a small amount of the rock powder was placed on a glass slide, slurried with acetone, the surface smoothed by hand, and allowed to dry. Later on in the study aluminum sample holders (see Appendix IC) were used to

Map 2 THE KIRKLAND LAKE-LARDER LAKE GOLD CAMP





(TIHOR)
1943)

2072

hold the powders rather than the glass slides. The aluminum holders allowed for the use of a consistent amount of sample and permitted a smoother powder surface to be prepared.

It was assumed that the crushing procedure homogenized the rock, therefore one aliquot of powder from each sample was analysed in the following manner. The sample was scanned from 50° to 60° of two theta at a rate of one degree per minute. The major diagnostic peaks of the minerals most likely to be present in the rock are within this range. The results were recorded on a chart recorder which ran at 2 centimeters per minute.

The two theta angle of each definite peak was measured and its d spacing calculated using Bragg's equation $\lambda = 2d \sin\theta$. With the d spacings it was possible to identify the various minerals using the Joint Commission of Powder Diffraction Standards Files (see Figure 2.1)

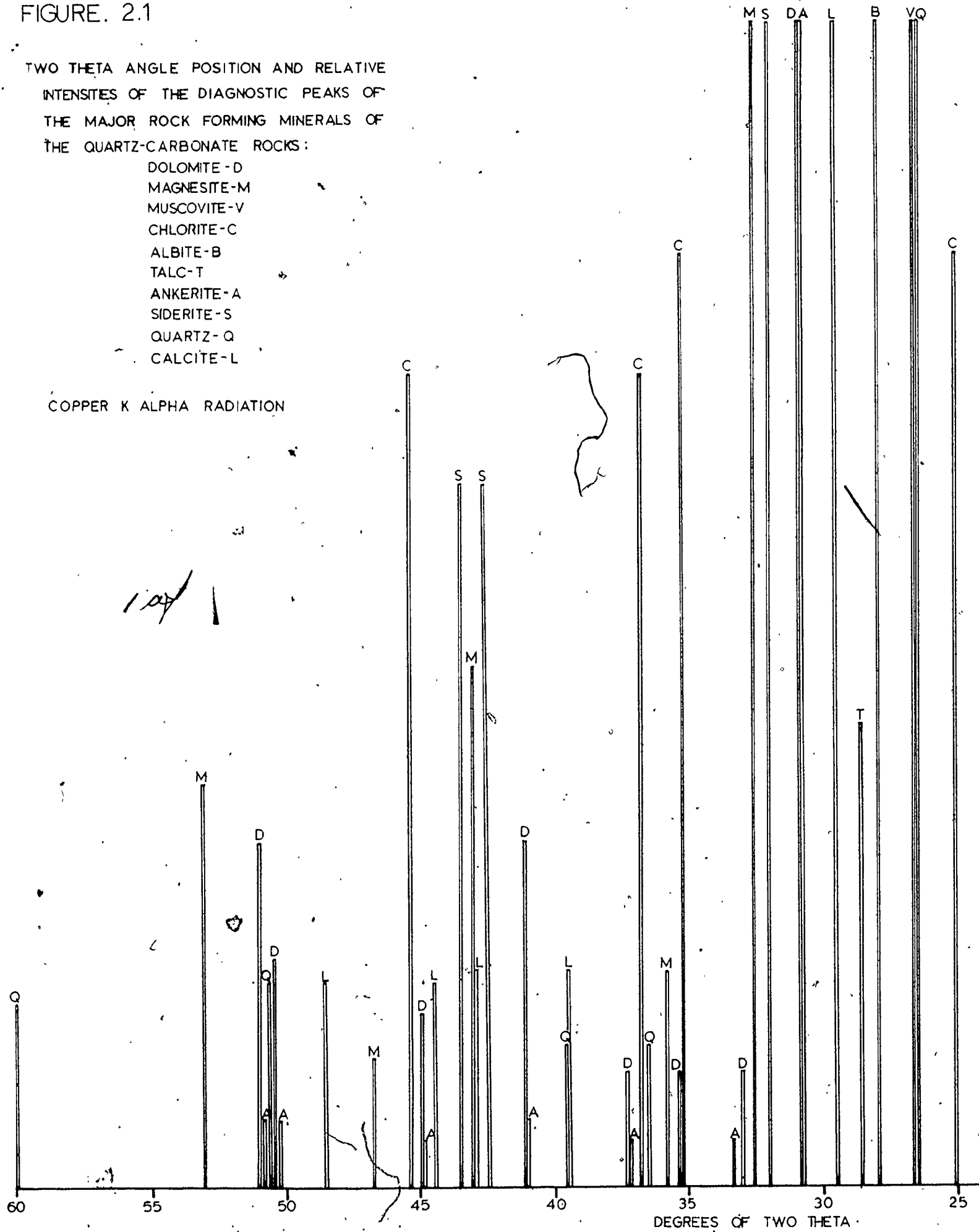
Quartz, dolomite and magnesite were by far the most common and prominent minerals present. A separate chart of each mineral was made using pure samples of each of the three minerals. Subsequent charts from each sample were compared with each pure mineral chart and the peaks representing quartz, magnesite and dolomite quickly noted and eliminated from further consideration. Finding the identity of the remaining peaks became easier with fewer peaks. The results of the whole rock powder scans of the samples are presented in Section 3.1.

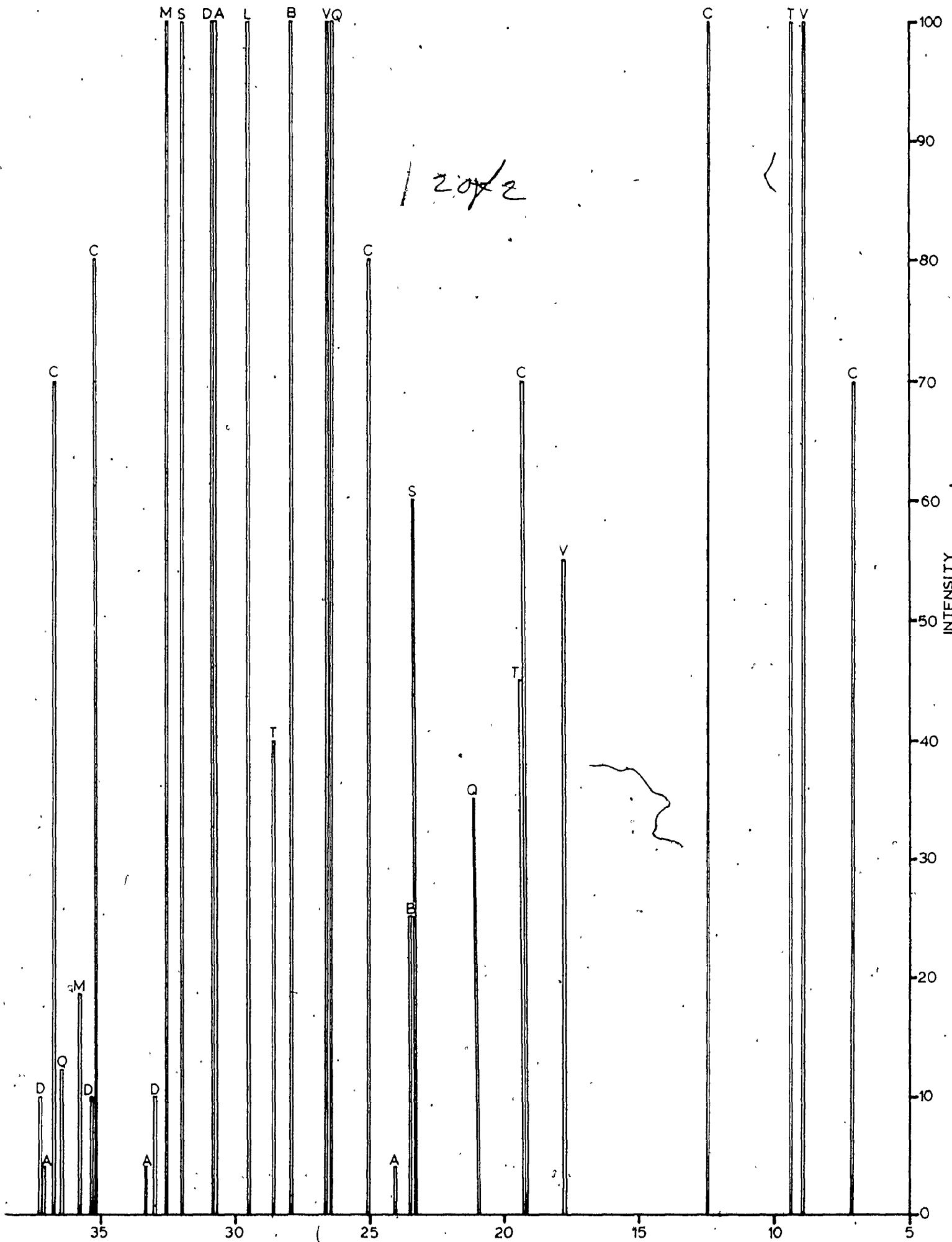
FIGURE. 2.1

TWO THETA ANGLE POSITION AND RELATIVE INTENSITIES OF THE DIAGNOSTIC PEAKS OF THE MAJOR ROCK FORMING MINERALS OF THE QUARTZ-CARBONATE ROCKS:

- DOLOMITE - D
- MAGNESITE - M
- MUSCOVITE - V
- CHLORITE - C
- ALBITE - B
- TALC - T
- ANKERITE - A
- SIDERITE - S
- QUARTZ - Q
- CALCITE - L

COPPER K ALPHA RADIATION





2.3 Quantitative Analysis of Carbonate Minerals by X-ray Diffraction

2.3.1 Introduction

Quartz, magnesite and dolomite are the dominant minerals in the quartz-carbonate rock. This fact was established early in the evaluation of the whole rock powder scans described in Section 2.2 above. The relative amounts of the three minerals were determined by comparing the peak height ratios of the samples to the peak height ratios of two series of prepared standards.

2.3.2 Standards - Preparation and Analysis

2.3.2.1 ST-1 to ST-9 Magnesite plus Dolomite

The first series of standards was prepared by combining magnesite and dolomite (see Appendix II) in ten percentile mixtures by weight. Each standard weighed 10 grams.

	ST-1	ST-2	ST-3	ST-4	ST-5	ST-6	ST-7	ST-8	ST-9
% M	10	20	30	40	50	60	70	80	90
% D	90	80	70	60	50	40	30	20	10

M - magnesite D - dolomite

The powders were placed in 5 dram glass vials and acetone was added to make a thick slurry. The mixture was stirred vigorously, by hand, over several minutes until it appeared smooth and even in colour (the magnesite powder was white and the dolomite powder was light brown). The vials were then left open to allow the acetone to evaporate. The dry mixture was stirred again before the slides were prepared for the x-ray diffractometer.

A small amount of powder was lightly packed into the rectangular opening of an aluminum sample holder. Five aliquots of

powder were taken from each standard and analysed in the following manner. To obtain sufficient precision the X-ray diffractometer was set to oscillate 5 times between 30° and 33° of two theta, to cover the d_{104} peak of dolomite at 2.886 \AA or 30.95° two theta and the d_{104} peak of magnesite at 2.742 \AA or 32.70° two theta with copper K alpha radiation. The results were recorded on a chart recorder.

The best fit background level was visually traced on the chart and the heights of the dolomite and magnesite peaks, above background, were measured. The peak heights were consistently measured from the background line to the top edge of the ink on the highest part of the peak. The peak height, was measured directly to the nearest millimeter and estimated visually to 0.1 mm.

The ratio D/M (peak height d_{104} dolomite/peak height d_{104} magnesite) was calculated, correct to 2 decimal places, for each oscillation and the five ratios averaged to find the mean of the aliquot. The means for the five aliquots were then averaged to obtain a grand mean for the standard.

The results of this First Powder Run of Standards ST-1 to ST-9 are presented in Table 2.1, and are presented graphically in Figure 2.2. The percentage error spread seemed rather broad and incomplete mixing of the powders was deemed the cause of the large variability in D/M ratio determinations. To improve the reproducibility the same powders were further mixed in acetone, dried, and analysed again using the methods described above. The results of the Second Powder Run of Standards ST-1 to ST-9 are presented in

Table 2.2. In the second run the limits of the standard field were reduced only marginally.

The results obtained were of sufficient precision to be useful for the purposes of this study, i.e. the semi-quantitative analysis of the rock powder samples. In the interest of developing a method that could be useful in obtaining a more precise quantitative identification of an intimate mixture of carbonates, the mixing problem was pursued further.

Two aspects to the mixing problems were important. The first was the straightforward problem of obtaining a homogenous blend of two different materials even though the two powders were ground to the same mesh size (-200). The second, and probably more significant problem is one that is often associated with carbonates and other minerals with good cleavage. It is extremely difficult to obtain a random orientation of grains in a mixture of such materials. It was realized that a medium was required that would suspend and separate the particles so that they could be mixed, and that would also act as a matrix to hold the particles in random orientation after the mechanical mixing was completed. White petroleum jelly (Vaseline) was chosen as the medium and was employed in the following manner.

The magnesite and dolomite powders were carefully weighed into glass vials and an approximately equal volume of melted petroleum jelly was added to each vial and the mixtures stirred as they cooled. The mixtures were remelted several times and the stirring action repeated. The magnesite powder tended to stay in clumps that were

Table 2.1

FIRST POWDER RUN OF STANDARDS ST-1 TO ST-9

- Acetone Slurry Preparation

D/M (height of Dolomite peak d₁₀₄ at 30.95° 2θ/height of Magnesite peak d₁₀₄ at 32.70° 2θ)

- copper K alpha radiation

Mean of Aliquot	1	2	3	4	5	GM	SD	%E
ST-1 D/M	16.05	14.91	14.81	14.53	16.14	14.69	1.87	12.74
ST-2 D/M	10.38	7.04	6.09	5.99	6.53	7.21	1.82	25.27
ST-3 D/M	4.54	5.01	3.90	3.85	3.48	4.16	0.61	14.69
ST-4 D/M	2.20	2.13	2.46	3.15	3.11	2.61	0.49	18.80
ST-5 D/M	1.97	1.53	1.64	2.18	2.22	1.91	0.31	16.35
ST-6 D/M	1.38	1.89	1.49	1.38	1.00	1.43	0.32	22.25
ST-7 D/M	0.71	0.97	1.14	0.63	0.55	0.80	0.25	30.87
ST-8 D/M	0.36	0.31	0.51	0.59	0.74	0.50	0.17	33.51
ST-9 D/M	0.14	0.14	0.17	0.09	0.17	0.14	0.03	23.36

GM-grand mean

SD-standard deviation

%E-percent error

Table 2.2 SECOND POWDER RUN OF STANDARDS ST-1 TO ST-9
 - Acetone Slurry Preparation

D/M (height of Dolomite peak d104 at 30.95° 2θ/height of Magnesite peak d104 at 32.70° 2θ)

- copper K alpha radiation

Mean of Aliquot	1	2	3	4	5	GM	SD	%E
ST-1 D/M	14.00	18.99	10.89	13.35	10.60	13.57	3.38	24.88
ST-2 D/M	4.52	7.75	5.68	7.16	7.33	6.49	1.35	20.79
ST-3 D/M	4.22	3.53	3.49	4.66	3.03	3.79	0.65	17.08
ST-4 D/M	2.25	1.96	3.40	2.34	2.82	2.66	0.57	2.14
ST-5 D/M	1.93	1.34	1.09	1.78	1.79	1.59	0.36	22.33
ST-6 D/M	1.39	1.42	1.54	1.34	0.78	1.29	0.29	22.84
ST-7 D/M	1.05	1.06	1.17	0.71	0.64	0.73	0.24	32.22
ST-8 D/M	0.79	0.44	0.66	0.40	0.55	0.57	0.16	28.11
ST-9 D/M	0.16	0.22	0.14	0.16	0.09	0.15	0.05	31.13

GM-grand mean
 SD-standard deviation
 %E-percent error

Table 2.3

THIRD POWDER RUN OF STANDARDS ST-1 TO ST-9

- Petroleum Jelly Preparation

D/M (height of Dolomite peak d104 at 30.950 2θ/height of Magnesite peak d104 at 32.70 2θ)

- copper K alpha radiation

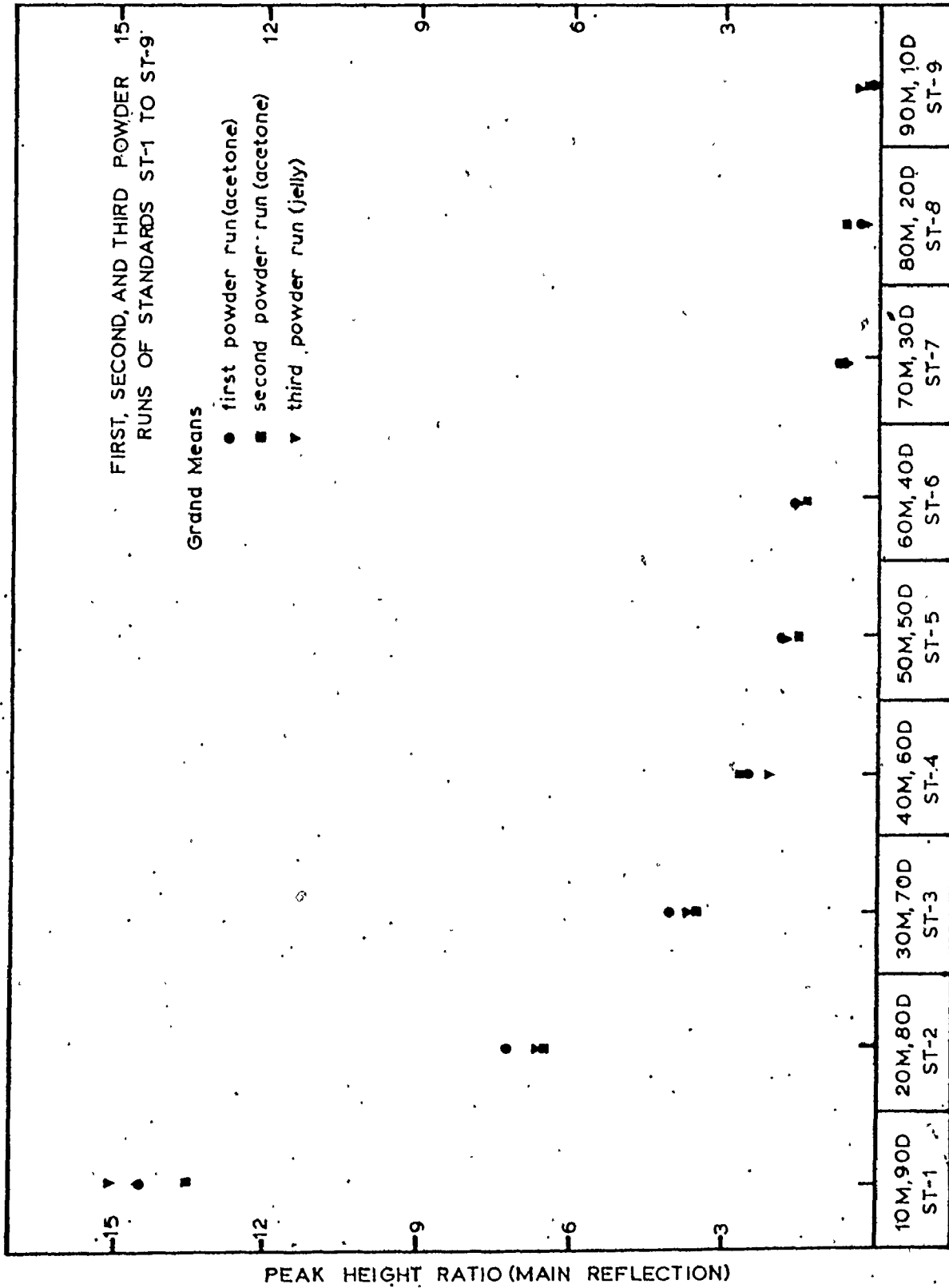
Mean of Aliquot	1	2	3	4	5	GM	SD	%E
ST-1 D/M	19.05	14.91	14.50	14.48	12.88	15.16	2.31	15.22
ST-2 D/M	6.97	6.59	6.69	6.59	6.42	6.69	0.20	3.05
ST-3 D/M	3.35	3.73	4.06	3.83	3.36	3.67	0.31	8.40
ST-4 D/M	2.07	2.41	2.14	2.19	2.18	2.20	0.13	5.80
ST-5 D/M	2.06	1.53	1.75	2.01	1.91	1.85	0.23	12.26
ST-6 D/M	1.12	1.50	1.56	1.38	1.53	1.42	0.18	12.68
ST-7 D/M	0.76	0.78	0.81	0.69	0.91	0.79	0.08	10.17
ST-8 D/M	0.44	0.39	0.50	0.49	0.46	0.46	0.04	9.55
ST-9 D/M	0.23	0.20	0.18	0.31	0.20	0.22	0.05	23.31

GM-grand mean

SD-standard deviation

%E-percent error

FIGURE 2.2



PERCENTAGE OF DOLOMITE(D) AND MAGNESITE(M) (BY WEIGHT)

difficult to break up with the stirring rod in the glass vials. Eventually the contents of each vial was emptied in turn into a large (6 inch) agate mortar and ground and stirred until a smooth, even texture was obtained. The mixing time required was about one half hour for each sample.

The results of the Third Powder Run of Standards ST-1 to ST-9 are presented in Table 2.3, and the grand means are plotted in Figure 2.2. The degree of homogeneity obtained using the petroleum jelly was far superior to that obtained with acetone. The variance for replicate measurement of mineral ratios was significantly smaller as reflected in the narrower percentage error spread. Using the petroleum jelly method in the standard magnesite-dolomite the percentage of magnesite could be determined to within about 10 percent.

It is interesting to note in Figure 2.2 that the ratio of the main peak heights of the two minerals are close to one only when the mixture contains 70% magnesite and 30% dolomite. The higher concentrations of dolomite are reflected in a disproportionately large peak. This is due to the greater scattering efficiency of the heavier calcium atom as compared to the magnesium atom.

2.3.2.2 ST-21 to ST-29 Magnesite plus Quartz

The second series of standards was prepared by combining magnesite and quartz in ten percentile mixtures by weight. Each standard weighed ten grams.

	ST-21	ST-22	ST-23	ST-24	ST-25	ST-26	ST-27	ST-28	ST-29
% Q	10	20	30	40	50	60	70	80	90
% M	90	80	70	60	50	40	30	20	10

Table 2.4

FIRST POWDER RUN OF STANDARDS: ST-21 TO ST-29

- Petroleum Jelly Preparation

Q/M (height of Quartz peak d101 at 26.85° 2θ/height of Magnesite peak d104 at 32.70° 2θ)

- copper K alpha radiation

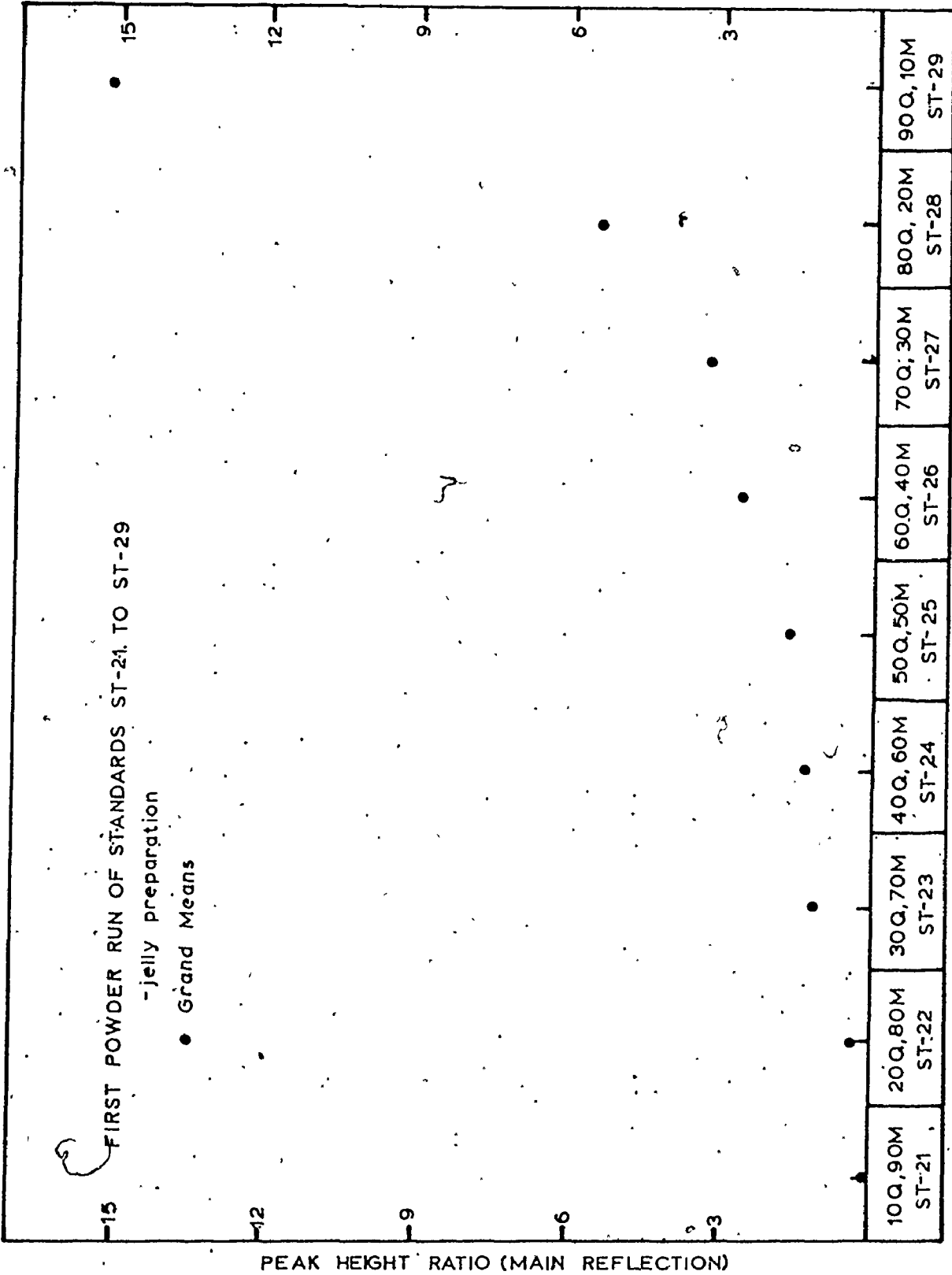
Mean of Aliquot	1	2	3	GM	SD	%E
ST-21 Q/M	0.17	0.15	0.20	0.17	0.03	14.80
ST-22 Q/M	0.48	0.32	0.44	0.41	0.08	20.31
ST-23 Q/M	1.46	0.87	1.18	1.17	0.30	25.22
ST-24 Q/M	1.21	1.43	1.15	1.26	0.15	11.70
ST-25 Q/M	2.01	1.53	1.56	1.70	0.27	15.82
ST-26 Q/M	2.73	2.31	3.02	2.69	0.36	13.27
ST-27 Q/M	3.65	3.81	2.93	3.46	0.47	13.55
ST-28 Q/M	5.44	5.70	5.58	5.57	0.13	2.34
ST-29 Q/M	11.18	12.25	22.53	15.32	6.27	40.91

GM-grand mean

SD-standard deviation

%E-percentage error

FIGURE 2.3



The powders were mixed using light petroleum jelly as described above. The X-ray diffractometer was set to oscillate between 26° and 33° two theta. The lower limit was set at 26° for this series of standards in order to cover the d_{101} peak of quartz at 26.85° with copper K alpha radiation.

The consistency of the ratios obtained when using the light petroleum jelly for standards ST-1 to ST-9 prompted the use of three oscillations over three aliquots for this set of standards.

The results of the First Powder Run of Standards ST-21 to ST-29 in light petroleum jelly are presented in Table 2.4 and the grand means are plotted in Figure 2.3. The percentage error spread is comparable to the jelly preparation run of ST-1 to ST-9.

2.3.3 Semiquantitative Analysis of Powdered Rock Samples

Once the percentage error spreads were finally established, it was possible to analyse each of the powdered rock samples to determine the percentages (by weight) of magnesite and dolomite in the carbonate fraction of the rocks, and the percentages of quartz and magnesite in the quartz plus magnesite fraction of the rocks. The rock powders were analysed in the following manner.

One aliquot of powder was mounted in an aluminum sample holder and placed in the X-ray diffractometer. The machine was set to oscillate five or three times between 26° and 33° of two theta. The samples were run in two groups as a result of continuing equipment breakdowns and lengthy repairs. The first group of 21 samples was run on the X-ray diffractometer at McMaster University. Five oscillations were employed in analysing this group.

The second and larger group of 28 samples was analysed on an X-ray diffractometer housed at the University of Toronto. Due to the consistent ratios obtained on the McMaster machine the number of oscillations was reduced to three. This maintained the precision and also had the advantage of an economy in time.

The peaks were measured and the ratios dolomite/magnesite and quartz/magnesite calculated. The five or three D/M and Q/M ratios were averaged and the standard deviations and standard errors calculated. The results of these analyses are presented in Table 3.2. With the means and standard errors it was possible to make a semiquantitative estimate of the weight percentages of dolomite, magnesite and quartz in the dolomite-magnesite-quartz portion of the rock. These estimates are correct to within about 20% on the average. The percentage error range may seem overly broad at first glance but the varied nature of the carbonates and the problems of obtaining representative samples in the field did not warrant a more precise estimate.

2.3.4 Interference with the Major Carbonate Peaks by the Quartz peaks

It was possible that the quartz peaks might interfere with the major peaks of the carbonate minerals. A series of standards were made up to test this possibility. Magnesite-dolomite mixtures from the ST-1 to ST-9 series were mixed with quartz to give magnesite-dolomite-quartz mixtures as shown in the table below.

Carbonate Standard	Carbonate/Quartz	Mineral % Mixtures		
		M	D	Q
ST-2				
M:D = 20:80	75:25	15	60	25
	50:50	10	40	50
	25:75	5	20	75
ST-5				
M:D = 50:50	75:25	37.5	37.5	25
	50:50	25	25	50
	25:75	12.5	12.5	75
ST-8				
M:D = 80:20	75:25	60	15	25
	50:50	40	10	50
	25:50	20	5	75

Three aliquots were taken from each standard and analysed in the diffractometer set to oscillate between 26° and 33°.

The various quantities of quartz did not effect the carbonate peak ratios. In all cases the D + M + Q mixtures D/M ratios remained similar to the accepted grand means for ST-2 ST-5 and ST-8.

2.4 Thin Sections

2.4.1 Transmitted Light Microscopy

A number of polished thin sections were prepared in order to make a preliminary evaluation of the effectiveness of thin section light microscopy in determining the mineralogy of the quartz-carbonate rocks. The rocks chosen for the thin section evaluation

were: EB-2, MV-2, MG-8, MG-7, OT-1, KA-1n, KA-4n, KA-12n and an unnumbered sample from the Kerr-Addison mine. The first five samples listed here represent outcrops from diverse locations and exhibit the variety of colours and textures encountered across the study area. The rocks prefixed KA are underground samples from the Kerr-Addison mine and were chosen as being representative of the quartz-carbonate ore in the mine. The unnumbered sample was selected to represent a unique area in the mine known locally as the "unaltered blocks" where the development of quartz stockwork and the effect of chloritic alteration has apparently not penetrated the rock. Blocks several inches across appear to be quite fresh. Thin section study was not pursued as a tool in identifying the minerals because of the higher degree of certainty of the X-ray diffraction method. The thin sections were most useful in exploring the textural relationships of the minerals and in identifying the minor amounts of sulphides and other opaque minerals that are present in quantities too small to be identified in the whole rock powder scans using the X-ray diffractometer.

2.4.2 Scanning Electron Microscopy (SEM)

As has been noted in Section 1.3 many of the earlier investigators in the Kirkland Lake-Larder Lake Gold Camp area allude to the presence of ankerite in the rocks. The ankerite pattern (see Figure 2.1) did not appear on any of the whole rock X-ray diffractometer scans. Chemical analyses show that the rocks can contain up to 10% iron (Ridler, 1969). The major purpose for using the SEM was to establish which mineral(s) contain the iron.

A number of polished thin sections were studied by the scanning electron microscope to obtain X-ray emission pictures. The portions of the slides to be analyzed were cut to the appropriate size (approximately 1 cm²), coated with carbon which acts as a conductor, and mounted for insertion into the specimen chamber.

Each element emits X-rays at specific energies when bombarded by an electron beam. By adjusting the detector windows, the X-ray emission(s) of a particular element can be isolated. The presence and intensity of the radiation is recorded and may be displayed digitally and visually. The visual records are in the form of Polaroid pictures where the various radiations are represented by white dots. The dot density is directly proportional to element concentration in the sample, but a similar concentration of two different elements will not necessarily produce the same concentration of dots. The results of the SEM analyses are presented in Section 3.3.2.

2.5 Mineral Staining

Mineral staining was evaluated as a method to identify the carbonate minerals and to determine their distribution within the rocks. To test the staining method, six slabs were cut from sample MG-11 which is typical of the quartz-carbonate ore from the Kerr-Addison mine. The slabs were treated using the method outlined in Figure 2.4.

The results of this exercise can only be described as an abject failure. Any portion of the slab, that was not massive quartz,

turned dark purple after the application of the Alizarin Red S plus 30% NaOH and remained in that state despite the use of any subsequent reagents.

The most likely explanation for this behavior is the complex carbonate mineralogy of the large recrystallized carbonate grains in the veins (see Section 4.3). The main mass of the rocks is a fine grained mixture of carbonate, quartz, chlorite and muscovite which will probably absorb the stains indiscriminately thereby making the results highly unreliable.

The staining technique was not pursued further because of these problems and because the results obtained from the X-ray diffractometer and the SEM are adequate to establish the carbonate mineralogy.

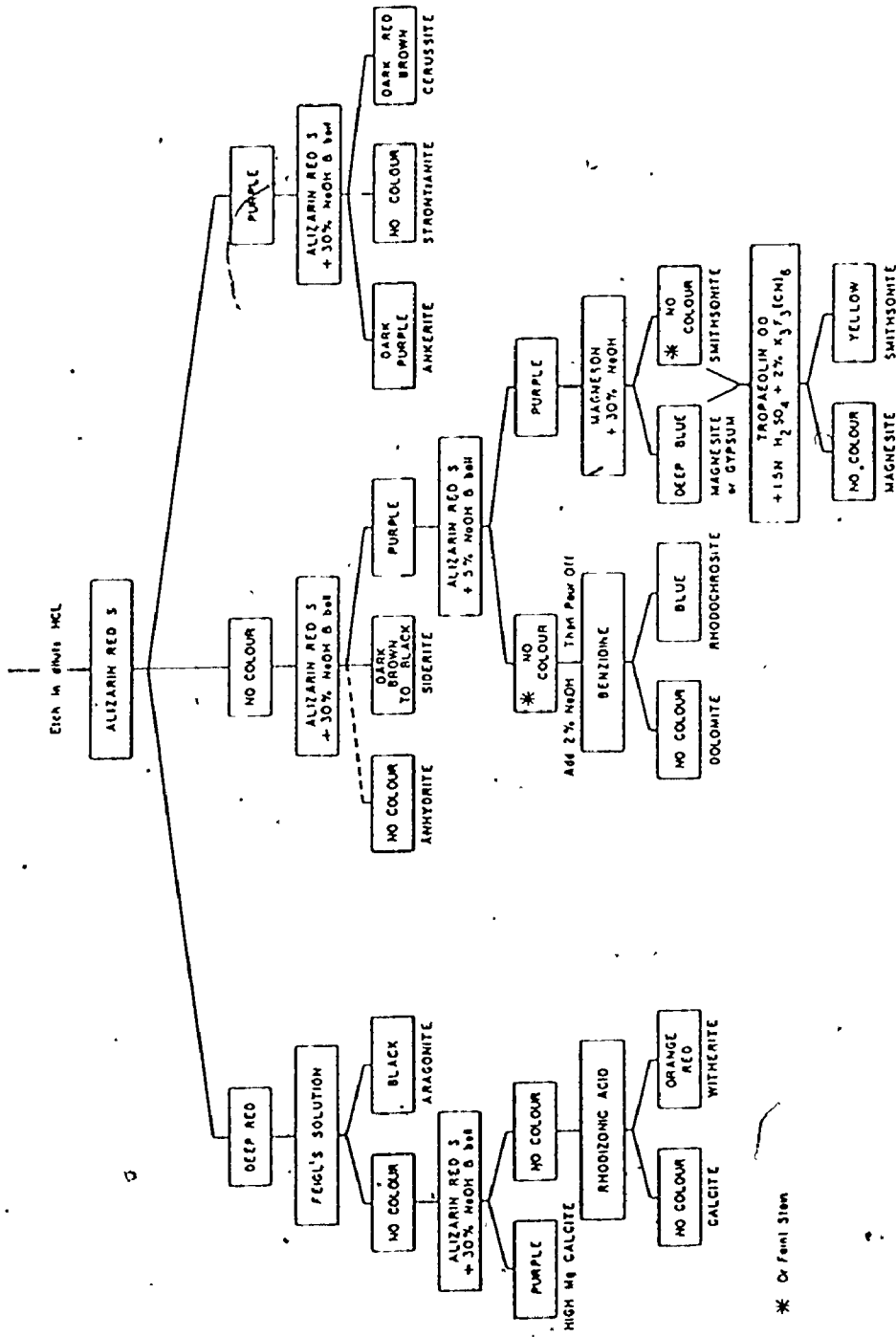


Figure 2.4 Staining scheme for carbonates in hand specimen and thin section (Hutchison, 1974 after Warne, 1962)

Chapter Three Results and Observations

3.1 Whole Rock Powder Scans

The peak heights of a single mineral as they appear on the whole rock X-ray diffraction scans are directly proportional to the amount of the mineral present in the sample. However, as shown in Figures 2.2 and 2.3 two minerals whose principal reflections result in similar main peak heights are not present in the rock sample in the same proportion.

The results of the whole rock powder scans are presented in Table 3.1 where the presence of the mineral is indicated. No attempt has been made to assign quantitative values to the mineral proportions.

3.2 Semiquantitative Analysis of Powdered Rock Samples

The ratios D/M (dolomite/magnesite) and Q/M (quartz/magnesite) were calculated from the peak heights for each of the rock samples which contained quartz, dolomite and magnesite. These data are presented in Table 3.2 and are also presented graphically in Figures 3.1 through 3.3 following. Figure 3.1 shows the proportion of magnesite with respect to the magnesite plus dolomite. Figure 3.2 shows the proportion of quartz with respect to quartz plus magnesite.

As has been noted in Section 2.3.3 above, the percentage error range is broad but the rock sampling did not warrant greater precision. In Figures 3.1 and 3.2 a line joining the grand means of the

Table 3.1

WHOLE ROCK POWDER SCANS FROM 5° TO 60° 2θ

31

SAMPLE	MINERALS PRESENT							D/M Q/M MAP#	FIELD DET. COLLECTOR
	QTZ	MAG	DOL	MUS	CHL	TLC	ALB		
MG-1	●		●	○				1	S. L. TIHOR
MG-2	●		●				●	2	"
MG-3	●		●		○			3	"
MG-4	●		●					4	"
MG-5	●	●	●	●				5	"
MG-6	●	●	●					6	"
MG-7	●	●		●				7	"
MG-8	●	●	●					8	"
MG-9	●	●	●		●			9	"
MG-303	●		●					10	L. A. TIHOR
MG-304	●	●	●					11	"
MG-305A	●	●	●					12	"
MG-305B	●	●	●					13	"
MG-305C	●	●	●					14	"
MG-305D	●	●	●					15	"
MG-306			●					16	"
MG-307	●		●					17	"
MG-309	●		●		●			18	"
MG-310	●	●	●					19	"
MG-311	●		●					20	"
MG-313			●		○			21	"
MG-314	●		●					22	"
MG-1003	●	●	●	●	●			23	"
MV-1	●		●	○			●	24	S. L. TIHOR

Table 3.1 (Cont.)

SAMPLE	QTZ	MINERALS PRESENT					TLC	ALB	MAP#	D/M	FIELD
		MAG	DOL	MUS	CHL	Q/M				COLLECTOR	
MV-2	●		●	●			●	25		S. L. TIHOR	
MV-3 1w	●				●		●	26		"	
MV-3 2w	●		●		●		●	27		"	
MV-4 1w	●		●		●			29		"	
MV-4 2w	●		●				●	30		"	
MV-4 3w	●		●		●			31		"	
MV-4 4w	●	●	●		○		●	32		"	
MV-4 5w	●	●	●		○		●	33		"	
MV-5 1e	●	●	●		●		○	34		"	
MV-5 2e	●	●	●				●	35		"	
MV-302	●	●	●					36		L. A. TIHOR	
MV-303	●		●					37		"	
MV-304	●		●					38		"	
MV-305	●		●				●	39		"	
MV-310	●		●		●			40		"	
MV-314A	●	●	●		●			41		"	
MV-314B	●	●	●		●			42		"	
MV-314C	●	●	●		●			43		"	
MV-315	●	●	●	●				44		"	
KA-1n	●	●	●	●	○		●	45		"	
KA-3n	●	●	●	●	●			46		"	
KA-4n	●	●	●	●	●			47		"	
KA-6n	●	●	●	●	●			48		"	
KA-8n	●	●	●	●	●			49		"	
KA-9n	●	●	●		●			50		"	
KA-12n	●	●	●	●	●			51		"	

Table 3.1 (Cont.)

SAMPLE	MINERALS PRESENT						ALB	MAP#	D/M Q/M DET.	FIELD COLLECTOR
	QTZ	MAG	DOL	MUS	CHL	TLC				
KA-15	●	●	●	○				52	L. A. TIHOR	
KA-25	●		●		●			53	"	
KA-35	●	●	●	●	●			54	"	
C-ORE	●	●	●					55	"	
GT-1A	●	●	●	●	●			56	S. L. TIHOR	
GT-2					●	●		58	"	
GAU-301	●	●	●	●				59	L. A. TIHOR	
GAU-308	●	○	●					60	"	
GAU-309	●	●	●	○	○			61	"	
SWA-6-11				●	●			62	"	
SWA-6-12			●	●	●			63	"	
SWA-6-13								64	"	
SWA-6-14	●		●			○	●	65	"	
SWA-6-15	●	●	●					66	"	
SWA-6-16	●		●				○	67	"	
EB-1	●		●		●			68	S. L. TIHOR	
EB-2	●		●		●			69	"	
EB-3	●	●	●				●	70	"	
EB-4	●		●	●	●		●	71	"	
EB-5A	●		●				●	72	"	
EB-5B	●	●	●	●				73	"	
EB-301	●	○					○	74	L. A. TIHOR	
TK-1	●	●	●					75	S. L. TIHOR	
TK-303	●	●	●		●			76-7	L. A. TIHOR	
TK-305	●		●				●	78	"	

Table 3.1 (Cont.)

SAMPLE	MINERALS PRESENT							ALB	MAP#	D/M	FIELD
	QTZ	MAG	DOL	MUS	CHL	TLC	Q/M			DET.	COLLECTOR
TK-306	●	●	●						79		L. A. TIHOR
709-9	●	●	●						80		"
709-11			●						81		"
709-12	●	●	●						82		"
709-13	●	●	●						83		"
MIS-4	●	●	●						84		"
DT1-7	●	●	●	●	○		○		85		"
LL-3	●	●	●	●	●				86		"
LL-9	●	●	●		●				87		"
LEB-302	●	●	●				●		88		"
FER-301	●	●	●	●					89		"
QUE-46-3	●	●	●		○				90		"
CH-302	●		●		●				91		"
OT-1	●		●				●		92		S. L. TIHOR
OT-2	●		●	●	●		●		93		"
OT-3	●	●	●		○				94		"

Note - QTZ-quartz, MAG-magnesite, DOL-dolomite, MUS-muscovite
 CHL-chlorite, TLC-talc, ALB-albite, D/M Q/M, DET.-ratios
 determined, MAP -map location number on map

- - mineral present
- - mineral may be present
- mineral absent

Table 3.2. SEMIQUANTITATIVE ANALYSES OF POWDERED ROCK SAMPLES

Map Location	Sample Number	Ratio	1	2	3	4	5	Mean	SD	%E
5	MG-51	D/M	0.64	0.80	0.71	0.68	0.89	0.74	0.10	13.51
		Q/M	2.01	2.34	2.20	2.01	2.53	2.22	0.22	10.04
5	MG-52	D/M	0.63	0.64	0.69			0.65	0.04	6.53
		Q/M	2.29	2.30	2.30			2.30	0.01	0.31
6	MG-6	D/M	0.67	0.71	0.73			0.70	0.03	4.40
		Q/M	2.96	2.98	2.73			2.89	0.14	4.80
7	MG-7	D/M	0.07	0.09	0.11			0.09	0.02	22.22
		Q/M	3.03	3.22	3.05			3.10	0.10	3.37
9	MG-9	D/M	2.06	3.19	2.93	3.00		2.79	0.50	18.00
		Q/M	4.84	4.64	5.04	3.72		4.56	0.58	12.79
11	MG-304	D/M	7.90	6.78	8.33	7.85	7.00	7.57	0.65	8.65
		Q/M	16.00	14.43	16.25	14.69	13.64	15.00	1.01	7.33
12	MG-305A	D/M	0.52	0.54	0.51			0.52	0.02	2.94
		Q/M	1.27	1.22	1.14			1.21	0.07	5.42
13	MG-305B	D/M	0.84	1.02	1.38			1.08	0.27	25.46
		Q/M	0.54	0.82	0.63			0.66	0.14	21.66

Table 3.2 (Cont.)

Map Location	Sample Number	Ratio	1	2	3	4	5	Mean	SD	%E
14	MG-305C	D/M	0.95	0.87	0.98			0.93	0.06	6.11
		Q/M	2.37	2.02	1.98			2.12	0.21	23.07
15	MG-305D	D/M	1.76	1.75	1.75			1.75	0.01	0.33
		Q/M	0.46	0.49	0.44			0.46	0.03	5.47
19	MG-310	D/M	1.10	1.08	1.18			1.12	0.05	4.72
		Q/M	1.06	1.56	1.18			1.27	0.26	20.55
23	MG-1003	D/M	0.10	0.15	0.18	0.23	0.09	0.15	0.06	38.59
		Q/M	0.25	0.34	0.27	0.40	0.11	0.27	0.11	40.45
33	MV-4-5w	D/M	1.12	1.15	1.19	1.18	1.00	1.13	0.08	6.78
		Q/M	9.40	9.16	9.13	8.76	8.59	9.01	0.33	3.63
36	MV-302	D/M	0.88	0.84	0.80			0.84	0.04	4.76
		Q/M	1.42	1.45	1.34			1.40	0.06	4.06
41	MV-314A	D/M	0.71	0.69	0.75			0.72	0.01	1.39
		Q/M	2.10	2.10	2.30			2.17	0.12	5.32
42	MV-314B	D/M	0.19	0.19	0.20			0.19	0.01	3.04
		Q/M	0.94	1.06	0.92			0.97	0.08	7.81

Table 3.2 (Cont.)

Map Location	Sample Number	Ratio	1	2	3	4	5	Mean	SD	%E
43	MV-314C	D/M	0.61	0.56	0.58			0.58	0.03	4.34
		Q/M	1.62	1.61	1.62			1.62	0.01	0.36
44	MV-315	D/M	0.89	1.02	1.02	1.04	1.03	1.00	0.07	6.90
		Q/M	1.43	1.67	1.53	1.75	1.79	1.63	0.14	8.78
45	KA-1n	D/M	7.06	4.96	7.70	8.08		6.95	1.39	20.03
		Q/M	7.80	5.44	7.00	7.40		6.91	1.03	14.95
46	KA-3n	D/M	0.54	0.89	0.67	0.46	0.62	0.64	0.16	25.45
		Q/M	0.68	0.53	0.45	0.58	0.58	0.56	0.08	14.97
47	KA-4n	D/M	0.58	1.00	0.63	0.72	0.87	0.76	0.17	22.85
		Q/M	1.00	1.08	1.05	1.18	1.08	1.08	0.07	6.09
48	KA-6n	D/M	0.42	0.41	0.41	0.47	1.03	0.55	0.27	49.20
		Q/M	0.25	0.31	0.23	0.36	0.39	0.31	0.07	22.16
49	KA-8n	D/M	0.65	0.42	0.50	0.35	0.38	0.46	0.13	28.01
		Q/M	0.49	0.49	0.64	0.46	0.48	0.51	0.07	14.23
50	KA-9n	D/M	1.42	1.51	1.56	2.25	1.67	1.68	0.33	19.65
		Q/M	1.96	2.04	1.68	1.71	1.66	1.81	0.18	9.76

Table 3.2 (Cont.)

Map Location	Sample Number	Ratio	1	2	3	4	5	Mean	SD	%E
51	KA-12n	D/M	11.75	4.83	18.00	7.00	3.41	9.00	5.94	66.02
52	KA-15	Q/M	13.25	3.92	10.00	6.88	3.41	7.49	4.16	55.55
		D/M	1.62	1.05	0.87	1.07	0.99	1.12	0.29	25.91
		Q/M	4.10	2.70	2.00	2.61	3.46	2.97	0.82	27.46
53	KA-25	D/M	11.67	11.32	15.00	12.08	9.50	11.91	1.99	16.68
		Q/M	7.67	8.52	11.30	6.75	8.33	8.51	1.70	20.03
54	KA-35	D/M	1.67	2.09	2.59	1.26	2.27	1.98	0.52	26.28
		Q/M	1.73	1.86	2.13	1.14	1.93	1.76	0.37	21.28
55	C-ORE	D/M	0.52	0.47	0.51			0.50	0.03	5.29
		Q/M	4.85	4.43	4.72			4.67	0.22	4.60
56	GT-1-A	D/M	0.26	0.22	0.24			0.24	0.02	8.33
		Q/M	0.94	0.91	0.81			0.89	0.07	7.65
59	GAU-301	D/M	0.90	0.98	0.96	0.77	0.84	0.89	0.09	9.73
		Q/M	1.02	1.00	1.09	1.02	1.06	1.04	0.04	3.49
61	GAU-309	D/M	1.17	1.24	1.29			1.23	0.06	4.90
		Q/M	1.06	1.09	1.10			1.08	0.02	1.93

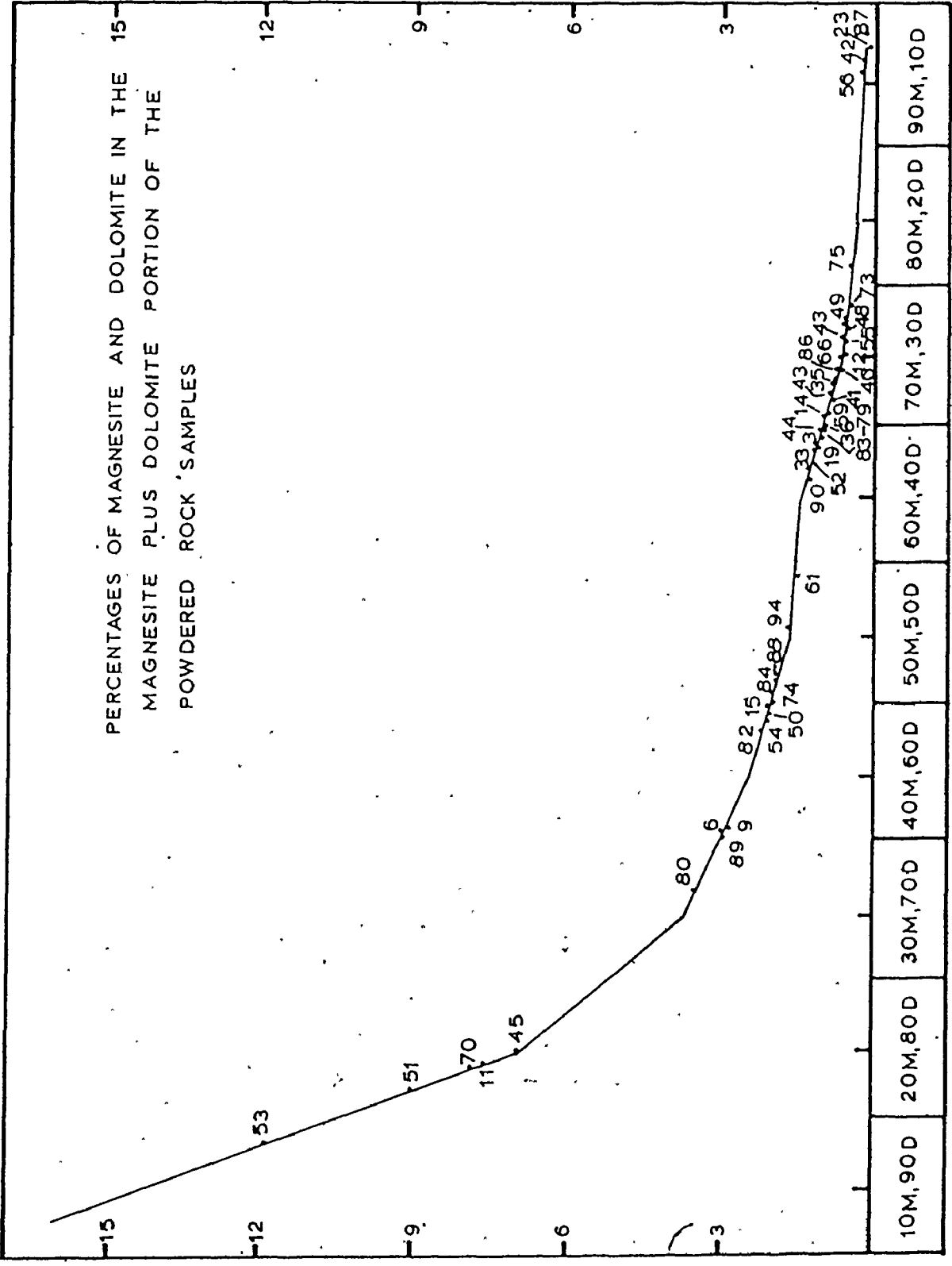
Table 3.2 (Cont.)

Map Location	Sample Number	Ratio	1	2	3	4	5	Mean	SD	%E
66	SWA-6-15	D/M	0.61	0.60	0.60			0.60	0.01	0.96
		Q/M	1.53	1.27	1.40			1.40	0.13	9.29
70	EB-3	D/M	6.00	9.20	8.17			7.79	1.63	20.97
		Q/M	5.25	7.00	5.83			6.01	0.89	14.83
73	EB-5-B	D/M	0.37	0.42	0.42	0.41	0.44	0.41	0.03	6.31
		Q/M	1.02	1.07	1.12	1.07	1.20	1.10	0.07	6.19
74	EB-301	D/M	1.60	2.30	2.10			2.00	0.36	18.03
		Q/M	24.40	40.10	33.40			32.60	7.88	24.17
75	TK-1	D/M	0.42	0.38	0.40	0.36	0.46	0.40	0.04	9.35
		Q/M	2.25	2.35	2.36	2.01	2.13	2.22	0.15	6.74
76	TK-303	D/M	0.49	0.52	0.48			0.50	0.02	4.16
		Q/M	1.73	1.62	1.73			1.69	0.06	3.76
79	TK-306	D/M	0.81	0.74	0.83			0.79	0.05	5.98
		Q/M	1.65	1.40	1.55			1.53	0.13	8.50
80	709-9	D/M	3.29	3.30	3.75			3.45	0.23	6.78
		Q/M	3.88	4.30	4.54			4.24	0.33	7.88

Table 3.2 (Cont.)

Map Location	Sample Number	Ratio	1	2	3	4	5	Mean	SD	%E
82	709-12	D/M	2.07	2.20	2.06			2.11	0.08	3.70
		Q/M	0.07	0.08	0.08			0.08	0.01	7.22
83	709-13	D/M	1.03	1.11	0.92			1.03	0.10	9.26
		Q/M	2.02	1.68	1.75			1.82	0.18	9.86
84	MIS-4	D/M	2.00	1.91	1.95			1.95	0.05	2.31
		Q/M	3.65	3.72	3.56			3.64	0.08	2.20
86	LL-3	D/M	0.67	0.39	0.58	0.68	0.58	0.58	0.12	20.07
		Q/M	1.69	1.06	1.52	2.06	1.92	1.65	0.39	23.62
87	LL-9	D/M	0.14	0.18	0.18	0.09	0.13	0.14	0.04	27.01
		Q/M	0.77	0.87	0.78	0.58	0.63	0.73	0.12	16.23
88	LEB-302	D/M	1.20	2.00	2.00			1.70	0.46	27.17
		Q/M	17.95	26.17	35.20			26.44	8.63	32.63
89	FER-301	D/M	2.74	2.73	3.27			2.91	0.31	10.62
		Q/M	2.14	1.41	2.98			2.18	0.92	42.25
90	QUE-46-3	D/M	1.15	1.20	1.27			1.21	0.06	4.98
		Q/M	2.04	2.29	2.24			2.19	0.13	6.04
94	OT-3	D/M	1.74	1.56	1.45	1.50	1.84	1.63	0.17	10.16
		Q/M	4.30	4.17	3.36	3.80	4.74	4.07	0.52	12.82

FIGURE 3.1

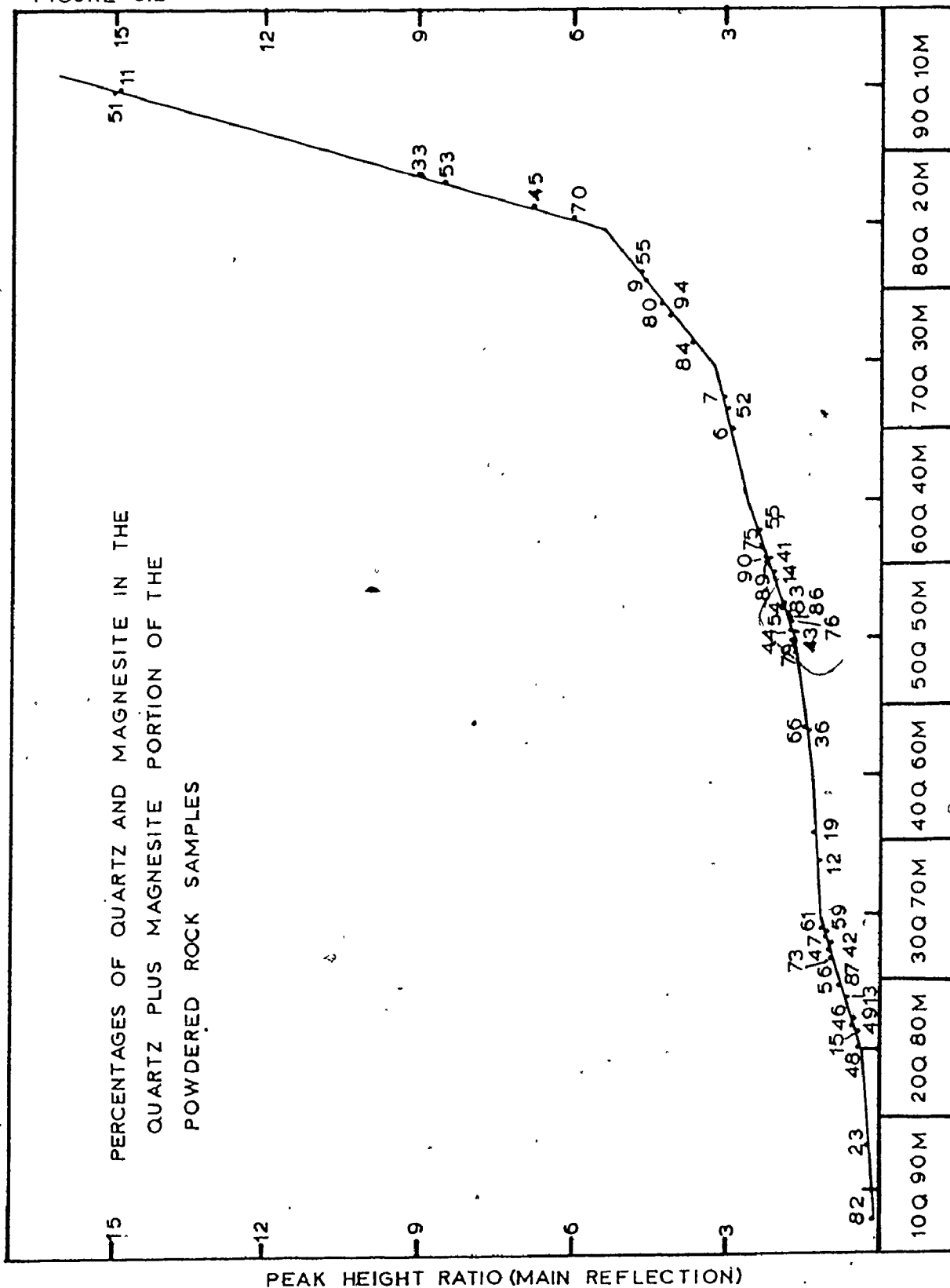


PERCENTAGES OF MAGNESITE AND DOLOMITE IN THE
MAGNESITE PLUS DOLOMITE PORTION OF THE
POWDERED ROCK SAMPLES

PERCENTAGE OF DOLOMITE(D) AND MAGNESITE(M) (BY WEIGHT)

PEAK HEIGHT RATIO(MAIN REFLECTION)

FIGURE 3.2



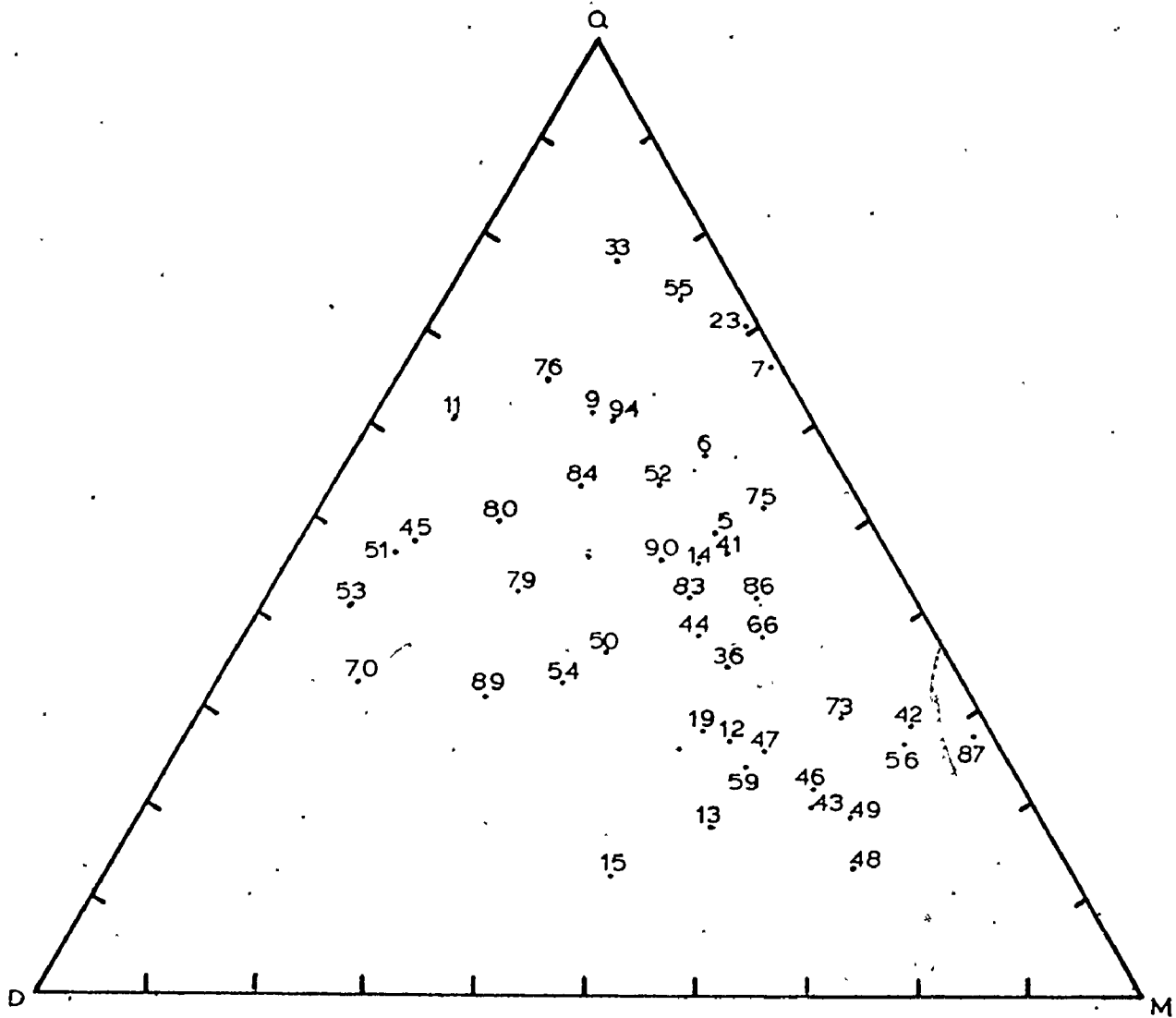
standard mixtures has been used as a standard curve for plotting the results of the whole rock powder scans. A mean obtained by averaging the peak height ratios of three or five oscillations may be plotted on the standard curve and a percentage content of dolomite-magnesite or quartz-magnesite read off the graph. The mineral percentages can be assumed to be correct to within about 20% for powder mounts. Samples mounted in vaseline may also be evaluated using these curves and the mineral percentages estimated to within about 10%.

Figure 3.3 is a triangular plot of the data from Figures 3.1 and 3.2, and Table 3.3 lists the approximate mineral percentages from Figure 3.3.

In the rock samples which contained all three of the dominant minerals, magnesite is the dominant carbonate in 75% of the rocks, generally making up over 50% of the carbonate fraction.

3.3 Thin Sections Transmitted Light Microscopy

The quartz-carbonate rocks show a great variety of colours and textures in hand specimen. The rocks are made up of a medium to fine grained variously coloured rock containing quartz and carbonate veins. The colours of the rocks sampled included light and dark beige, light grey, dark grey, dark green and a very bright green. Quartz veins are virtually always present and range from few and small to large and numerous. In some parts of the study area there is a fine interlayering of the white quartz and coloured quartz-carbonate portions of the rock. In other areas the coloured



PERCENTAGES OF QUARTZ, DOLOMITE, AND MAGNESITE

FIGURE 3.3

Table 3.3

APPROXIMATE MINERAL PERCENTAGES

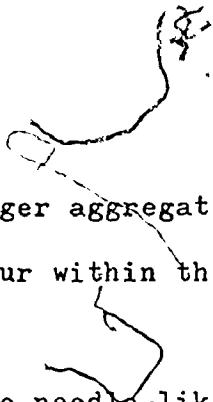
MAP	SAMPLE	%D	%M	%Q	MAP	SAMPLE	%D	%M	%Q
5	MG-5	15	35	50	53	KA-25	50	10	40
6	MG-6	10	35	55	54	KA-35	35	30	35
7	MG-7	<5	35	65	55	C-ORE	5	20	75
9	MG-9	20	20	60	56	GT-1-A	10	65	25
11	MG-304	30	10	60	59	GAU-301	25	50	25
12	MG-305A	25	50	25	61	GAU-309	30	45	25
13	MG-305B	30	50	20	66	SWA-6-15	15	45	40
14	MG-305C	20	35	45	70	EB-3	55	10	35
15	MG-305D	40	45	15	73	EB-5B	15	55	30
19	MG-310	25	35	30	75	TK-1	10	40	50
23	MG-1003	<5	30	70	76	TK-303	20	15	65
33	MV-4-5w	10	15	75	79	TK-306	35	20	45
36	MV-302	20	45	35	80	709-9	35	15	50
41	MV-314A	15	40	45	83	709-13	20	40	40
42	MV-314B	5	65	30	84	MIS-4	25	20	55
43	MV-314C	20	60	20	86	LL-3	15	40	45
44	MV-315	20	40	40	87	LL-9	5	70	25
45	KA-1n	40	10	50	89	FER-301	45	25	30
46	KA-3n	25	55	20	90	QUE-46-3	20	35	45
47	KA-4n	20	55	25	94	OT-3	20	20	60
48	KA-6n	20	65	15					
49	KA-8n	15	65	20					
50	KA-9n	30	35	35					
51	KA-12n	40	10	50					
52	KA-15	15	30	55					

portion of the rock is highly brecciated and the quartz forms a matrix.

In this study the emphasis was on collecting all of the variations of the quartz-carbonate rock, rather than a suite of samples that would reflect both the varieties and their relative abundances across the study area. A truly representative collection of samples would be very difficult to collect due to the great variety of quartz carbonate rocks across the study area and even across a single outcrop.

The minerals identified in thin section are quartz, carbonates, mica, chlorite, pyrite, and possibly leucoxene and rutile. The rock textures observed in the thin sections studied are remarkably similar whereas the hand samples from which the sections were cut are quite dissimilar in physical characteristics.

In thin section the rocks are consistently seen to be composed of a mass of fine grained quartz, carbonate, mica and/or chlorite and exhibit a massive to banded or schistose texture. The banded texture takes the form of short, narrow, undulatory lenses. The main mass of the rock, as described above, is cut by quartz and/or carbonate veins of various widths (Plate 3.1). Small opaque grains are disseminated throughout the main rock mass and occur infrequently in the quartz and/or carbonate veins. These grains are generally small and equigranular (Plate 3.2) but occasionally a much larger grain is present (Plate 3.3). The cubic morphology suggests they are pyrite. A rare mineral occurs as globular masses and is best observed with oblique light. Its colour ranges from light to dark



yellow. The larger aggregates occur in the quartz veins and the smaller ones occur within the rock mass proper. This mineral may be leucoxene.

Very fine needle-like grains make up a common accessory mineral of the main mass of the rock and were observed in most of the sections as fine scattered clusters. Occasionally they appear in greater concentrations along a particular micaceous band in the main rock mass. A few larger needles are present as infrequent clusters of grains and are bright red in crossed polars. The mineral was identified as rutile which was subsequently confirmed by SEM.

The variety of mica visible in the rock mass is too fine grained for a positive microscopic identification. The results of the X-ray diffraction studies show the mica to be muscovite. The bright green colour of the mineral indicates the mica is Cr rich fuchsite. This was not positively confirmed by the SEM results. The chlorite is also very fine grained and ranges in colour from dark green to black.

As has been reported in Section 3.1 feldspar is an important constituent of these rocks and was detected in a number of samples. None of these samples, unfortunately, were included in the thin section study. X-ray diffraction indicates that albite is present in sample MV-2 and therefore it should be a recognizable mineral in thin section. It was, however, not recognized and the author concludes that the albite is part of the fine grained matrix of the rocks and as such would be essentially impossible to distinguish from quartz.

It will be noted that in this discussion the author has so far not referred to specific carbonate minerals but has utilized the simple term "carbonate". The reason for the use of this terminology is that the specific carbonate minerals are very difficult to identify in thin section. Since the carbonate minerals are readily identified by X-ray diffraction no great effort was made to pursue thin section identification.

There seems to be some disagreement in the literature as to the twinning character of magnesite. Morehouse (1959) suggests that magnesite and dolomite may be distinguished by their twinning patterns, but then goes on to quote Rogers and Kerr (1942) who state that magnesite is never twinned. The textures encountered in the large carbonate grains in the veins in rocks from the study area would complicate the question of identification even further in that it is not uncommon to see a large carbonate grain which is partially twinned, i.e. twinned on one part of the grain and not on the other (Plate 3.4). Cross cutting twinning patterns can also be seen in Plate 3.4.

Quartz occurs in a variety of grain sizes. Undulatory extinction is ubiquitous in the quartz in both the veins and the main mass of the rock (Plate 3.1).

The large quartz grains that occur in some of the veins are rather unique, and interesting, in that the strain patterns in the quartz as manifested in the undulatory extinction are sometimes confined to a single grain or may cross many grains. One particularly striking pattern observed shows a concentric movement of

extinction in a poly-crystalline grain. The pattern looks almost like an explosion as the mineral is rotated on the microscope stage. (Plate 3.5).

Some of the quartz grains in the veins contain fluid inclusions. The inclusions are minute in size and are generally visible only under high power (400x). The shape of the inclusions varies, but they may generally be described as oblong capsules. Almost all of the inclusions contain a moving bubble. The movements of the bubble most often range from a stationary vibration to a slow wandering about the inclusion. Occasionally an inclusion contains a small bubble which moves at a very high speed, making many circuits of the inclusion in a few seconds.

Some of the quartz grains in the veins contain inclusions of tiny carbonate rhombs, and some much finer material that gives the quartz a dirty appearance. The "dirty" quartz grains are in the minority and are scattered among other quartz grains which are very clean.

The veins display a wide range of sizes. Some are very narrow carbonate or quartz veins made up of a single chain of grains, the same size as those in the main mass of the rock. Others are large massive quartz and/or carbonate veins many inches across in hand sample. Even small veins often contain quartz and carbonate grains large enough to be visible macroscopically.

The contacts between the veins and host rock are generally very sharp; however, some instances were observed where the contacts were gradational from the veins into the host rock. The center of

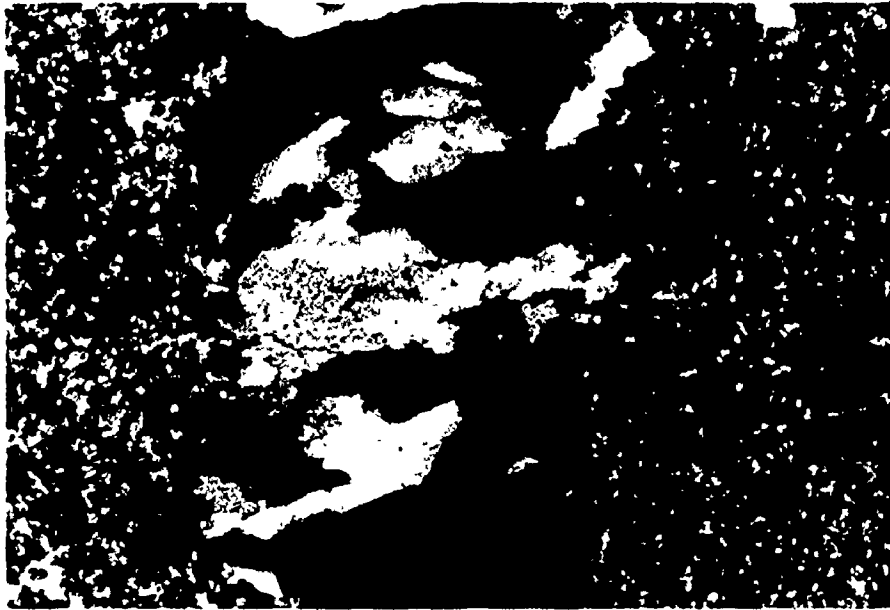


Plate 3.1 Quartz vein 25x crossed polarizers

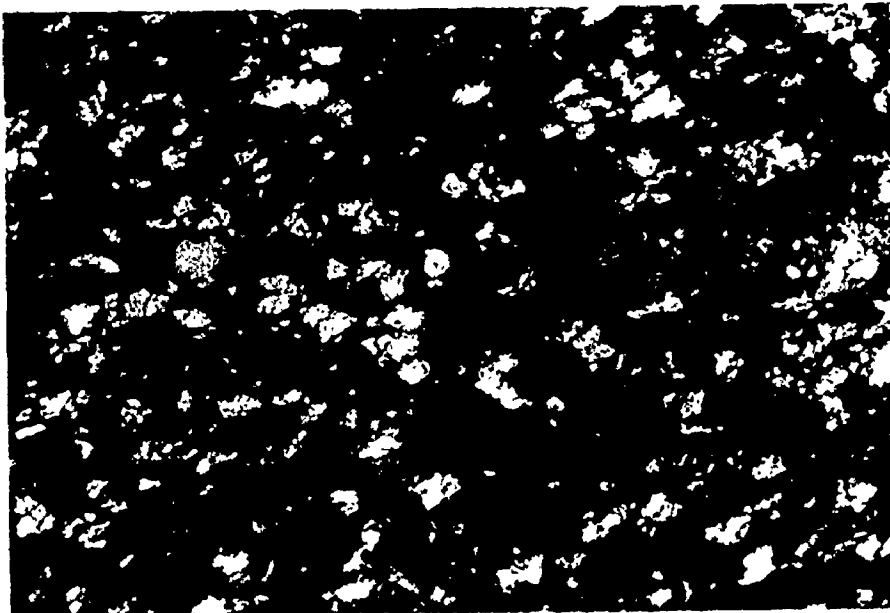


Plate 3.2 Massive green quartz-carbonate 25x
crossed polarizers



Plate 3.3 Pyrite grain in mica band 25x crossed polarizers :

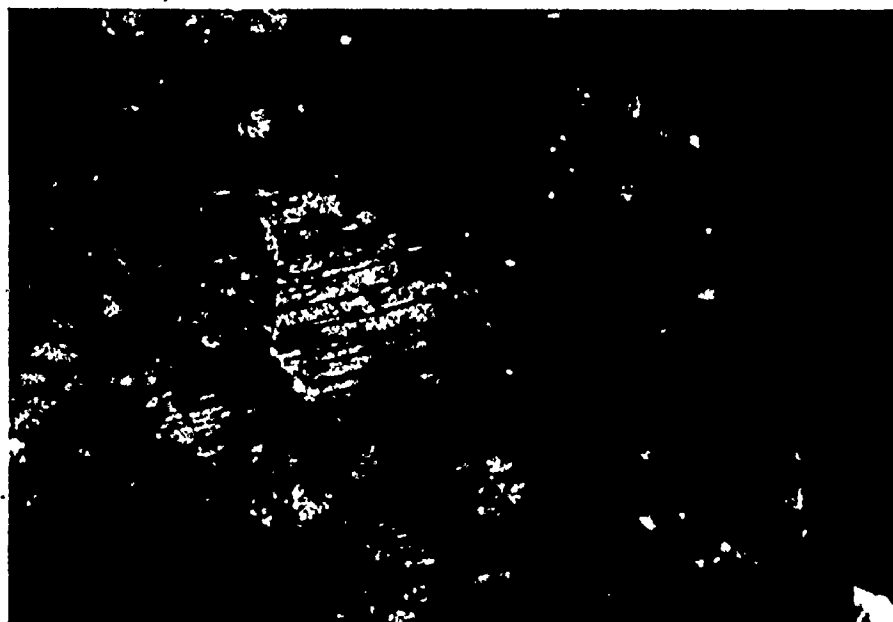


Plate 3.4 Twinning patterns in vein carbonates 25x crossed polarizers



Plate 3.5 Strain patterns in polycrystalline quartz grains 25x crossed polarizers

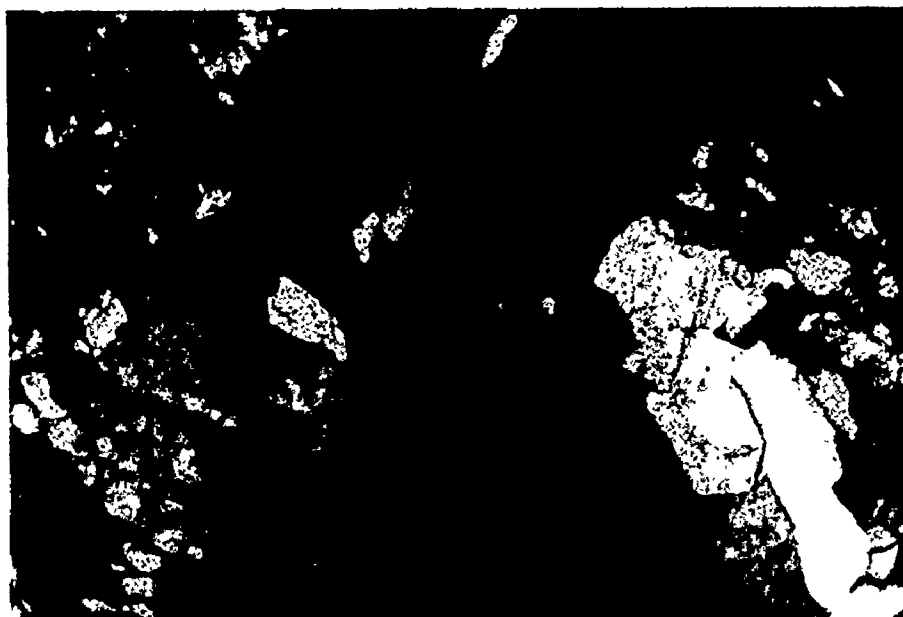


Plate 3.6 Twinning and recrystallization patterns in vein carbonates 25x crossed polarizers

the veins often consist of quartz with a thin selvage of carbonate along the contact with the host rock. Often both quartz and carbonate occur in a variety of grain sizes and morphologies in a single vein (Plate 3.6).

3.4 Thin Sections Scanning Electron Microscope (SEM, Stereoscan)

The distribution of iron in the rocks represented by the polished thin sections is very effectively resolved using the Stereoscan (SEM). The X-ray emission scans also provided more information than was originally anticipated in that they confirmed the presence of the accessory minerals that were concluded to be present as a result of the thin section studies described in Section 3.3.1, and also indicated the presence of some entirely unexpected minerals. The Stereoscan technique is especially useful at magnifications higher than those obtainable with light microscopy and aids greatly in the identification of the minerals in very fine grained rocks.

The following plates of the X-ray emission scans of rocks from the study area illustrate some of the results from the instrument and are a good indication of how useful the technique can be. This technique is not a definitive method on its own but used in conjunction with the light microscopy, X-ray diffractometry and a few chemical analyses it has helped to resolve some of the problems which arose during the completion of this thesis study. The data obtained from Plates 3.7 to 3.13 is summarized on Table 3.4.

Plate 3.7 shows a section from sample EB-2 and illustrates the fine grained nature of the major mass of the quartz-carbonate

Table 3.4

SUMMARY OF THE SUBJECT AND INTERPRETATION OF PLATES 3.7 TO 3.13

Sample	Plate	Subject	Interpretation
EB-2	3.7A	Electron image 5000x	
Area 1	3.7B	Si distribution	-quartz and other silicates
	3.7C	Al "	aluminosilicates
	3.7D	K "	
	3.7E	Fe "	
	3.7F	Mg "	-dolomite
	3.7G	Ti "	-rutile
	3.7H	Cr "	
EB-2	3.8A	Electron image 2000x	
Area 2	3.8B	Mg distribution	-dolomite and/or magnesite
	3.8C	Fe "	-dolomite and/or ankerite
	3.8D	Ca "	-dolomite
MG-11	3.9A	Electron image 50x	
Area 1	3.9B	Si distribution	-quartz
	3.9C	Ca "	-dolomite
	3.9D	Mg "	-dolomite and, magnesite
	3.9E	Fe "	-ankerite and/or chlorite
MG-11	3.10A	Electron image 1050x	
Area 2	3.10B	Si distribution	-quartz and other silicates

Table 3.4(Cont.)

Sample	Plate	Subject	Interpretation
	3.10C	Al distribution	-aluminosilicate--feldspar
	3.10D	K "	-feldspar
MV-2	3.11A	Electron image 50x	
	3.11B	Mg distribution	-dolomite
	3.11C	S "	-sulphide, possibly pyrite
	3.11D	Fe "	-pyrite
	3.11E	Ca "	-dolomite
EB-2	3.12A	Electron image 50x	
Area 3	3.12B	Si distribution	-quartz
	3.12C	Ba "	-barite
	3.12D	S "	-pyrite and barite
	3.12E	Ca "	-dolomite
	3.12F	Mg "	-dolomite
	3.12G	Fe "	-pyrite
EB-2	3.13A	Electron image 1000x	
Area 4	3.13B	Si distribution	-quartz
	3.13C	Ca "	-dolomite
	3.13D	Al "	-feldspar
	3.13E	Ti "	-rutile
	3.13F	Fe "	-pyrite
	3.13G	Mg "	-dolomite
	3.13H	P "	-apatite?



Plate 3.7A EB-2 Area 1 500x Electron image

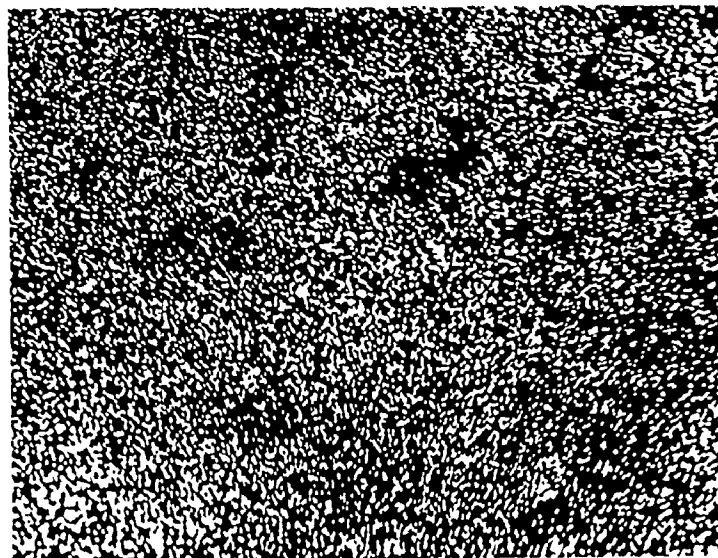


Plate 3.7B Si distribution

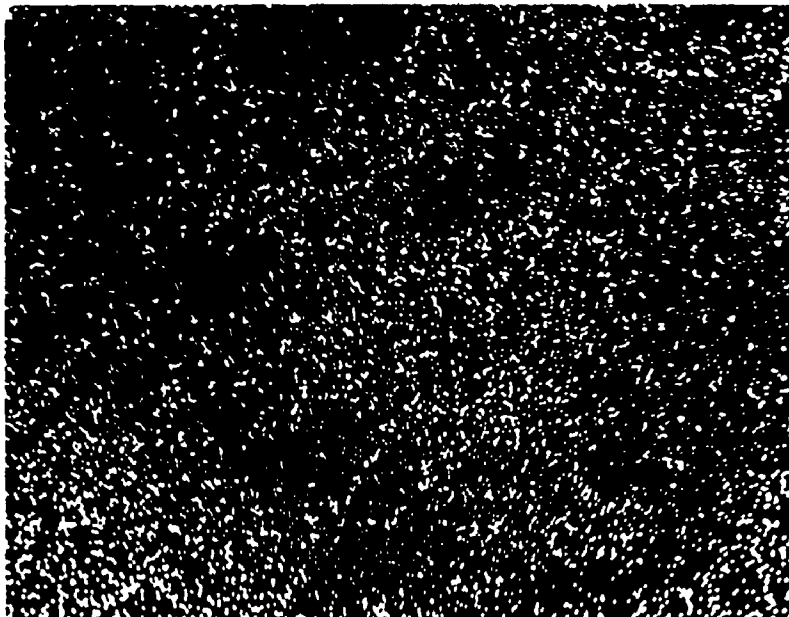


Plate 3.7C Al distribution

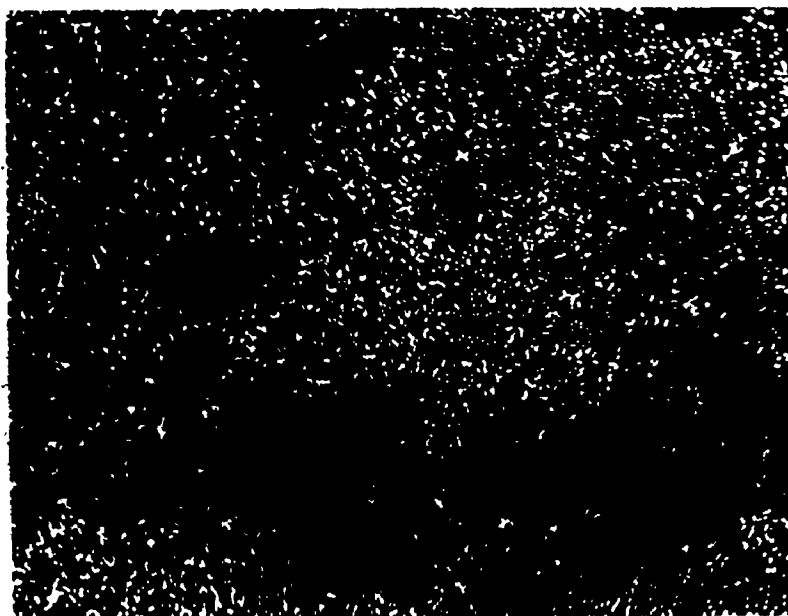


Plate 3.7D K distribution

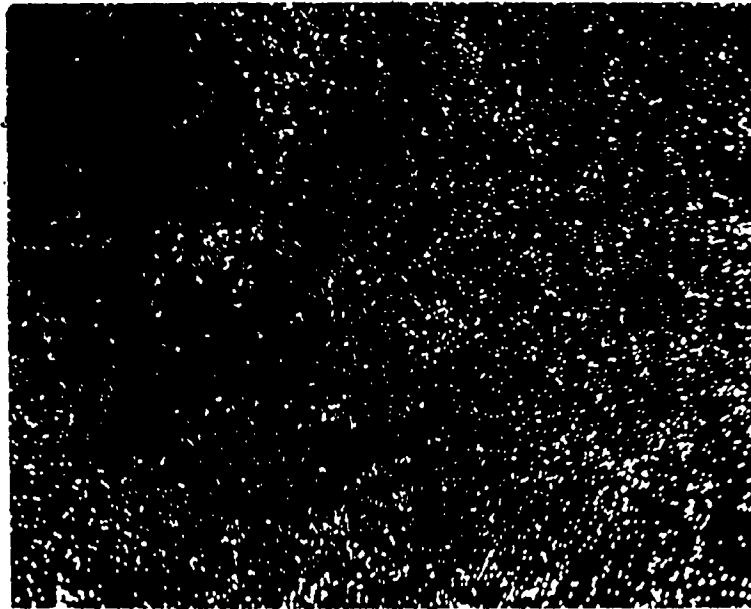


Plate 3.7E Fe distribution



Plate 3.7F Mg distribution



Plate 3.7G Ti distribution



Plate 3.7H Cr distribution

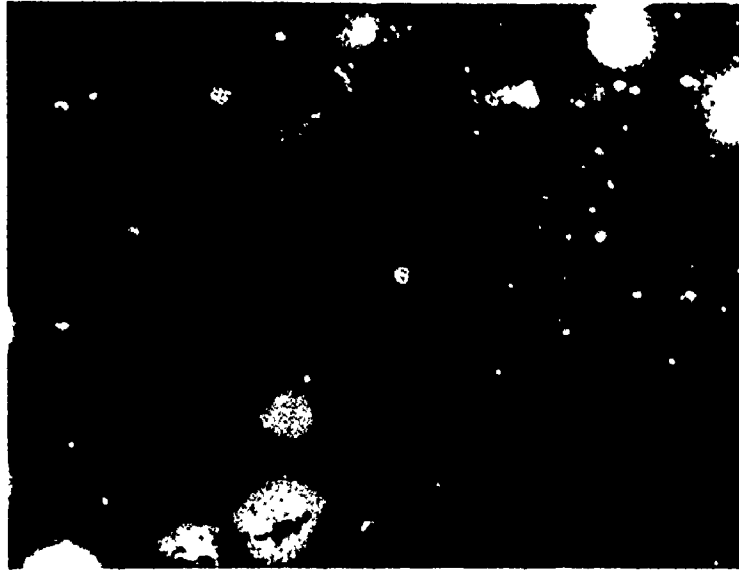


Plate 3.8A EB-2 Area 2 2000x Electron image



Plate 3.8B Mg distribution

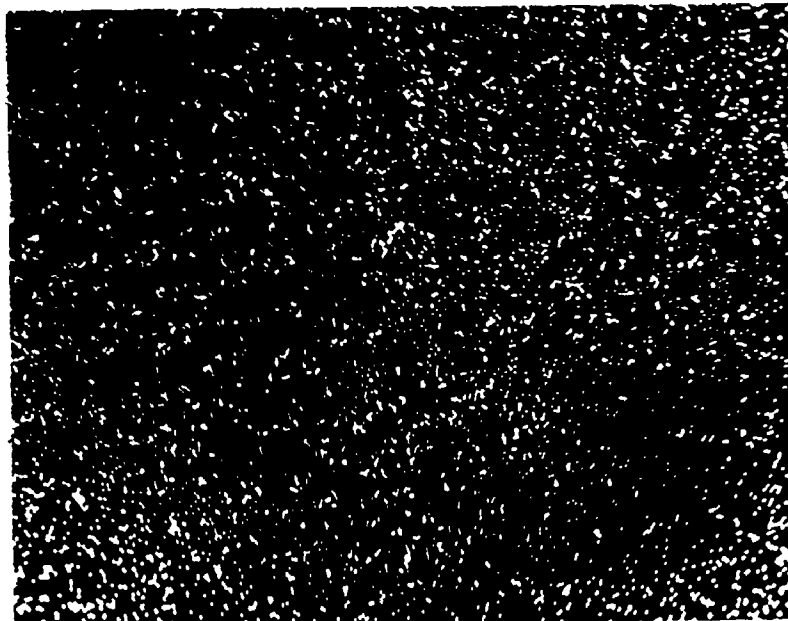


Plate 3.8C Fe distribution

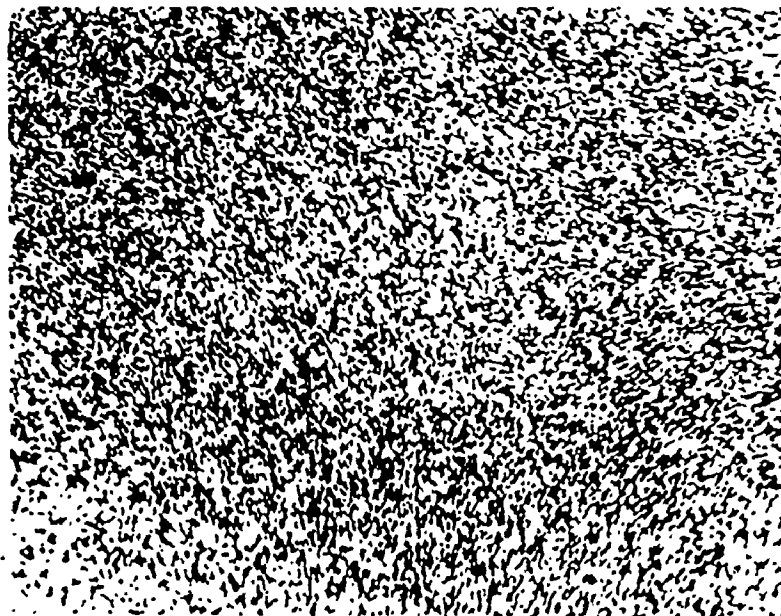


Plate 3.8D Ca distribution

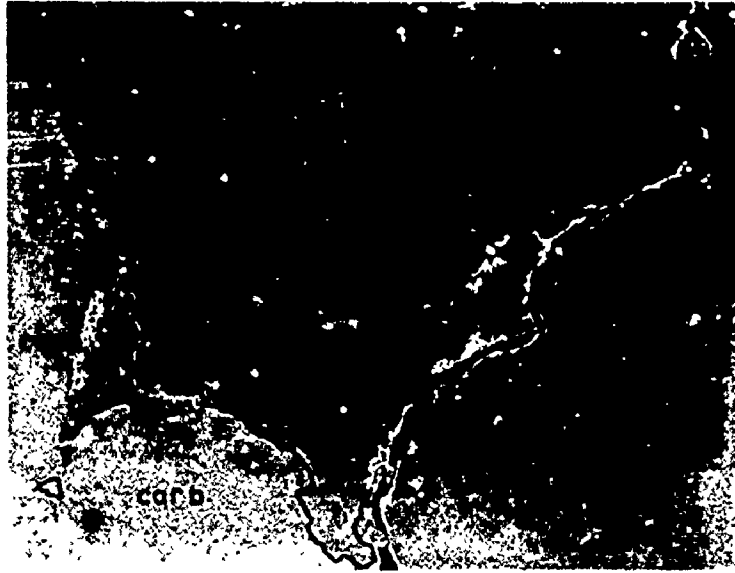


Plate 3.9A MG-11 Area 1 50x Electron image



Plate 3.9B Si distribution

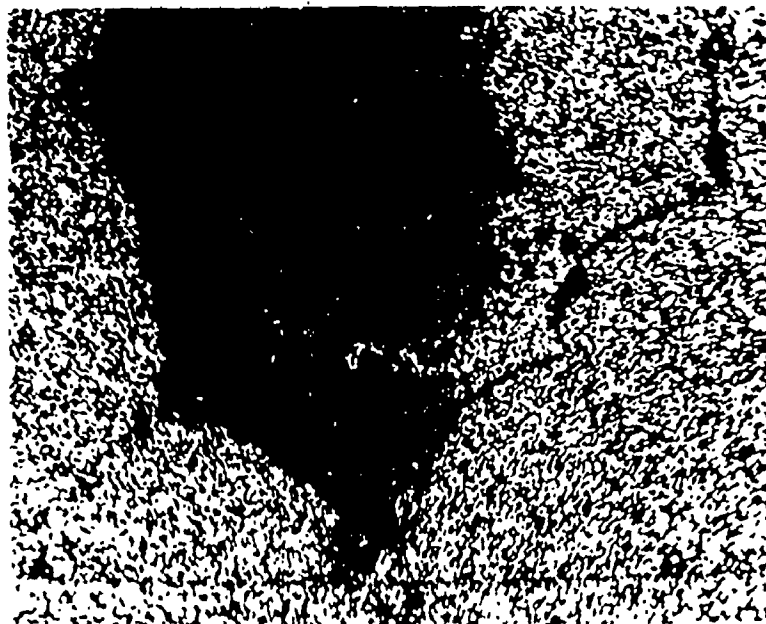


Plate 3.9C Ca distribution



Plate 3.9D Mg distribution

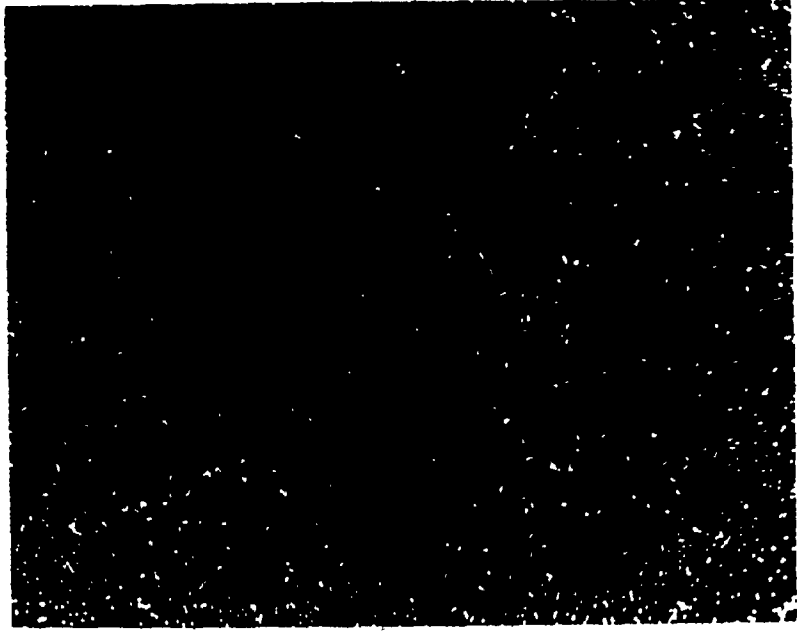


Plate 3.9E Fe distribution

12-3-5

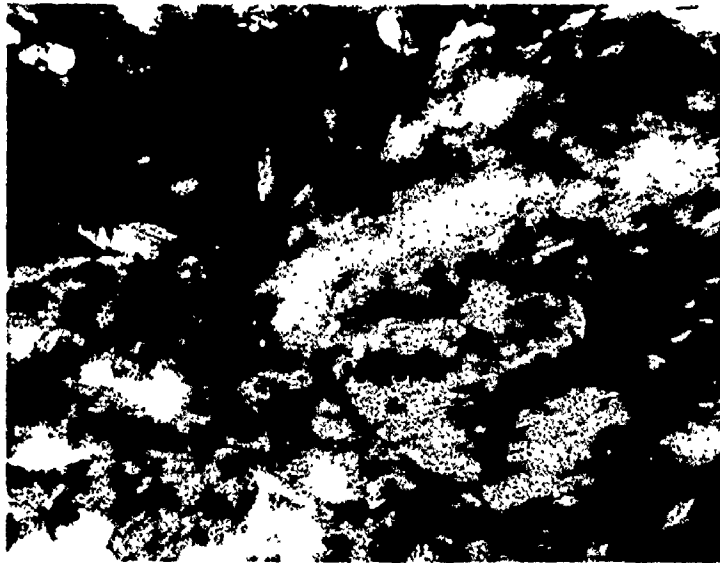


Plate 3.10A MG-11 Area 2 1050x Electron image

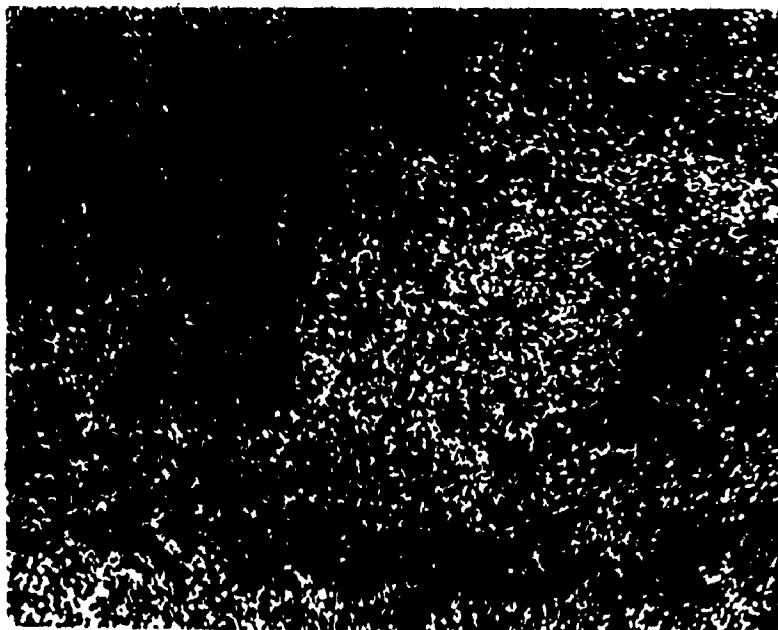


Plate 3.10B Si distribution

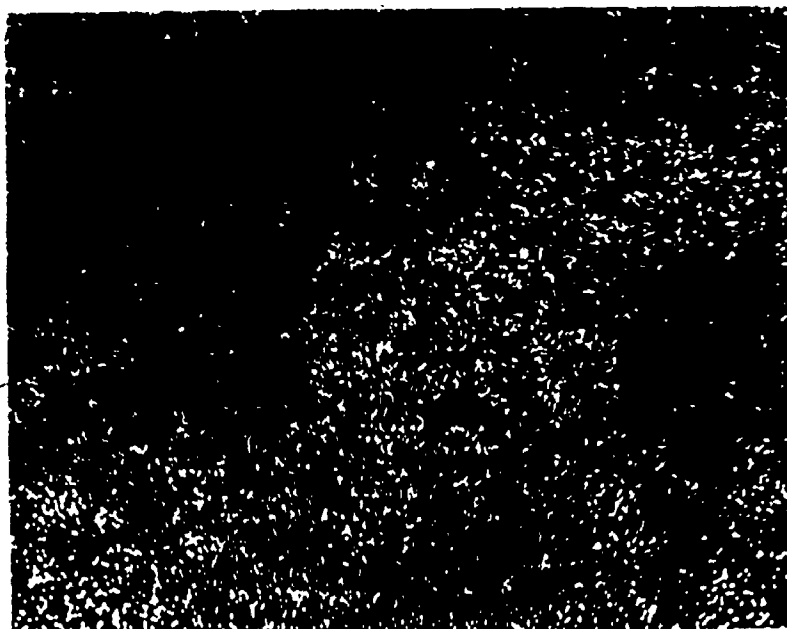


Plate 3.10C A1 distribution



Plate 3.10D K distribution



Plate 3.11A MV-2 50x Electron image

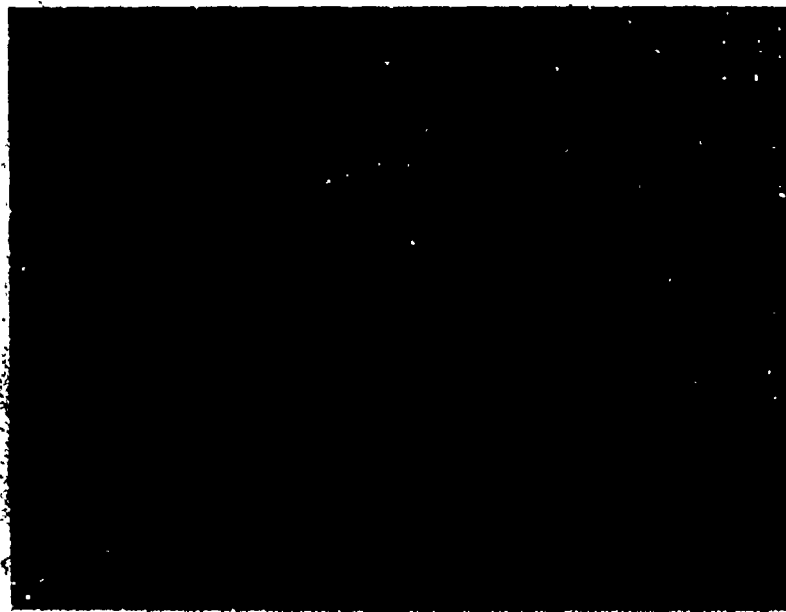


Plate 3.11B Mg distribution



Plate 3.11C S distribution



Plate 3.11D Fe distribution

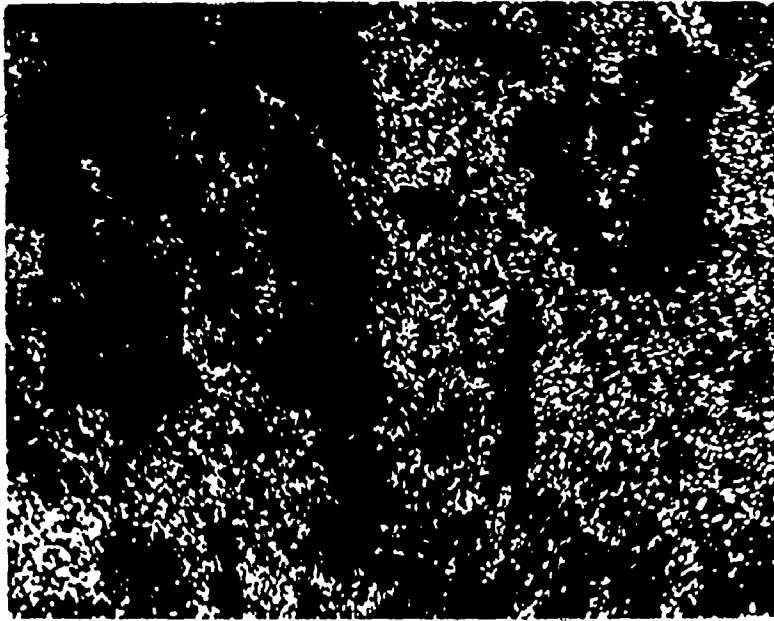


Plate 3.11E Ca distribution

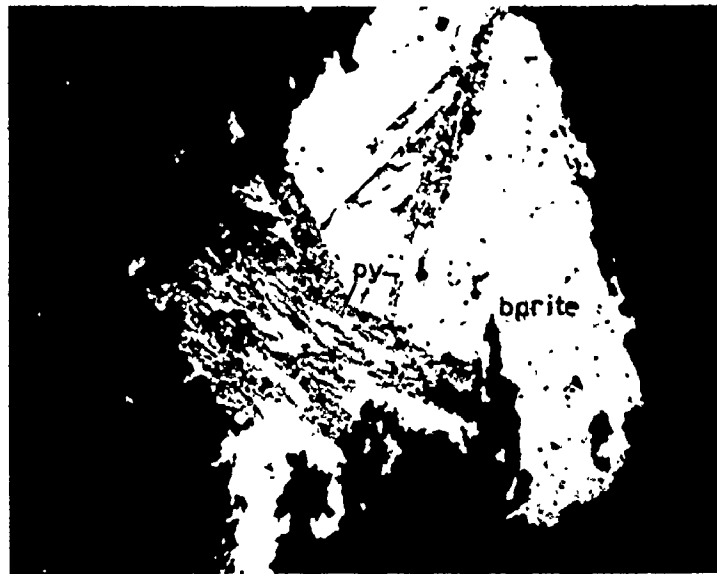


Plate 3.12A EB-2 Area 3 50x Electron image

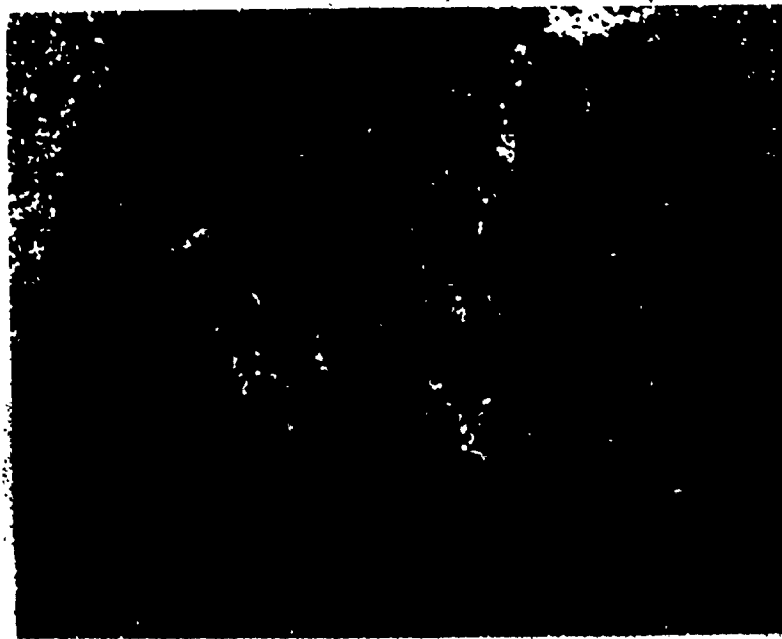


Plate 3.12B Si distribution

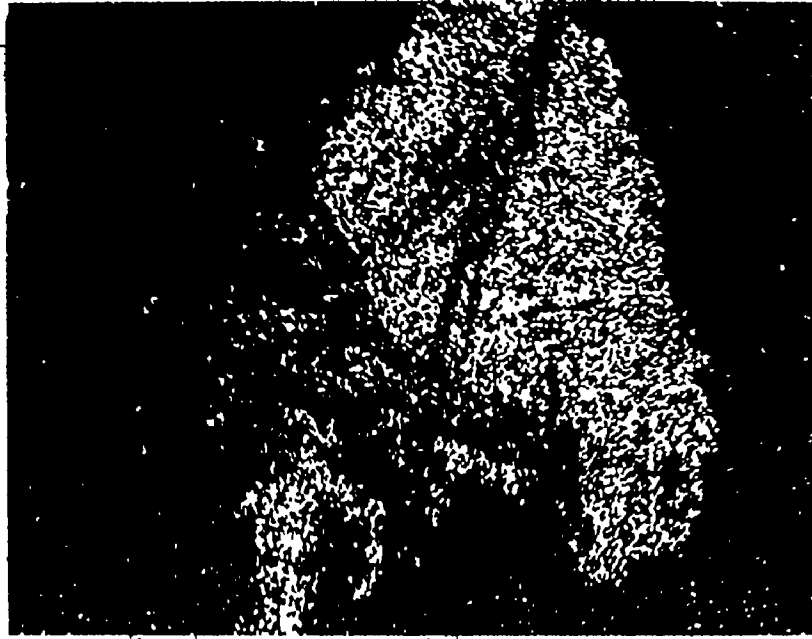


Plate 3.12C Ba distribution

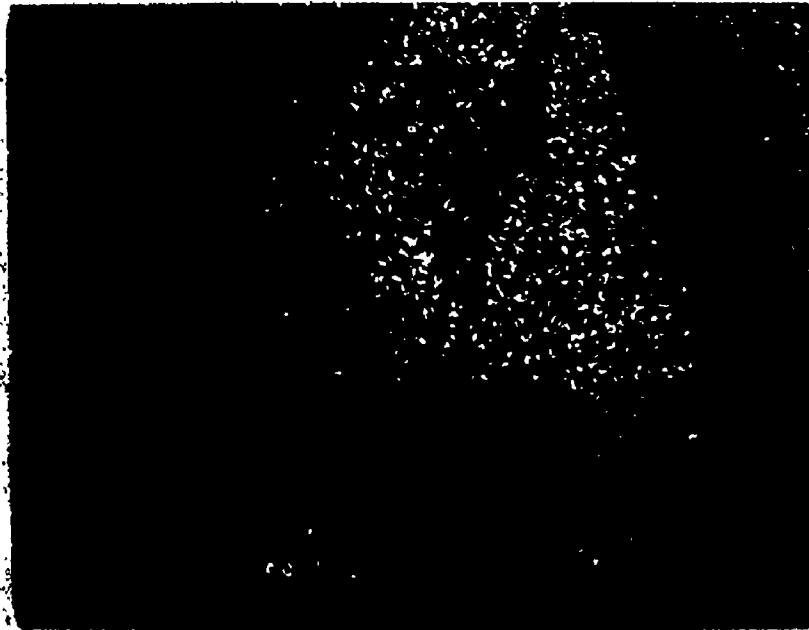


Plate 3.12D S distribution



Plate 3.12E Ca distribution



Plate 3.12F Mg distribution

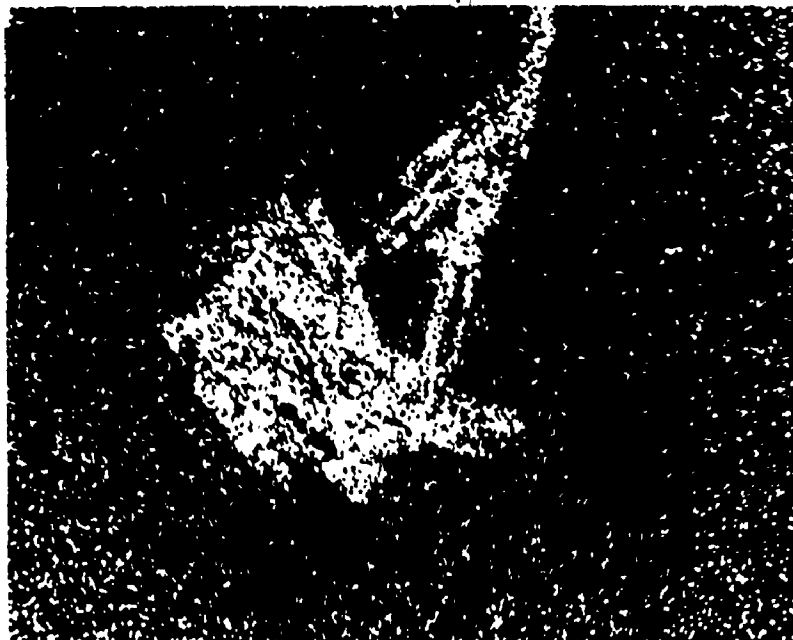


Plate 3:12G Fe distribution

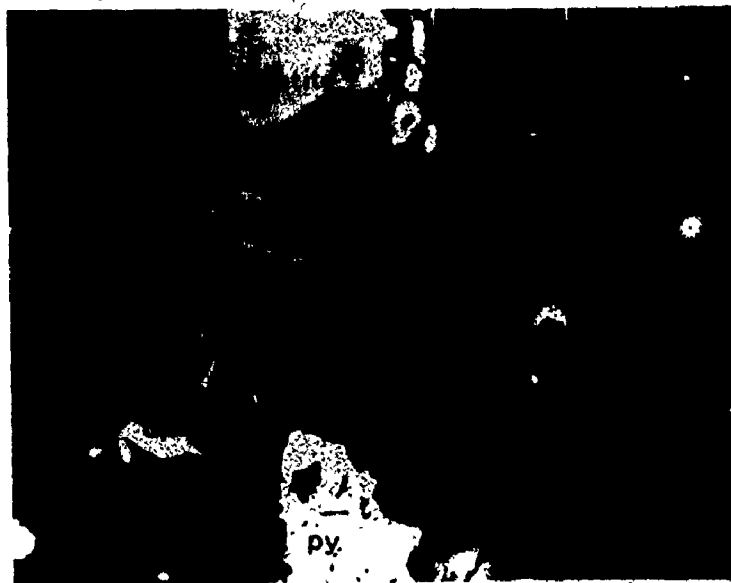


Plate 3.13A EB-2 Area 4 1000x. Electron image



Plate 3.13B Si distribution

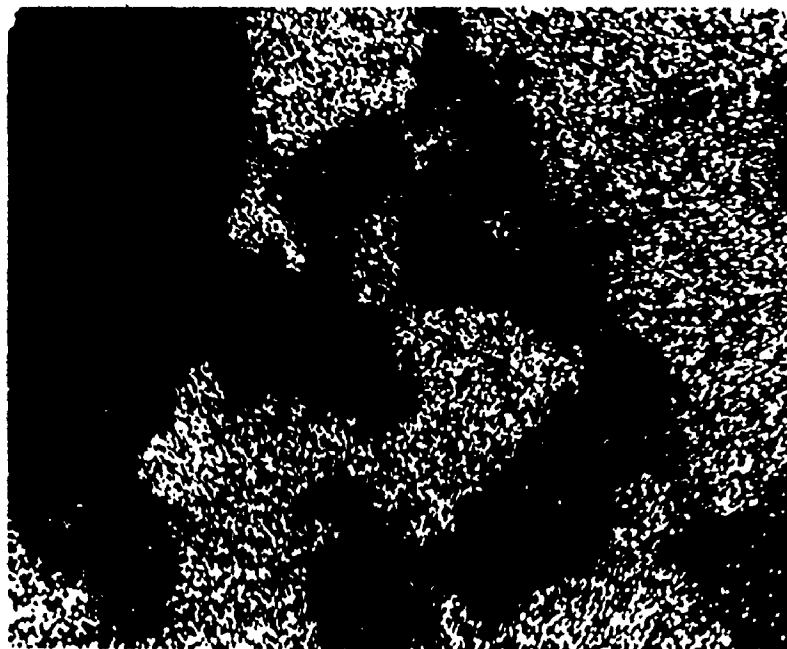


Plate 3.13C Ca distribution



Plate 3.13D Al distribution

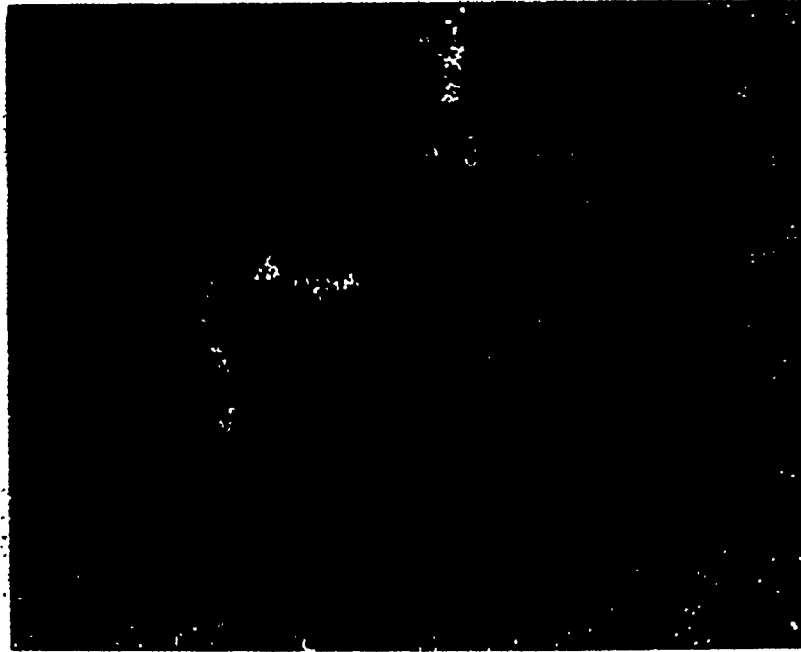


Plate 3.13E Ti distribution

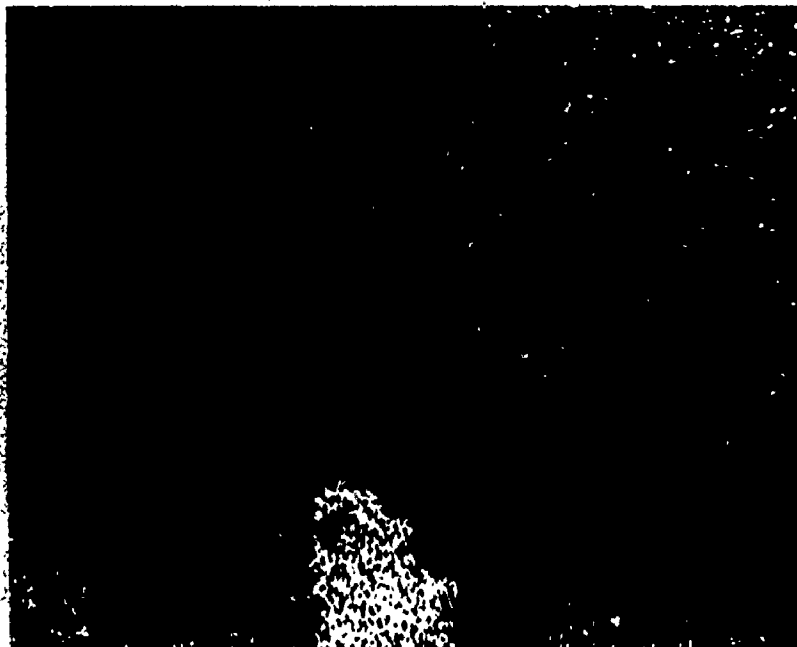


Plate 3.13F Fe distribution

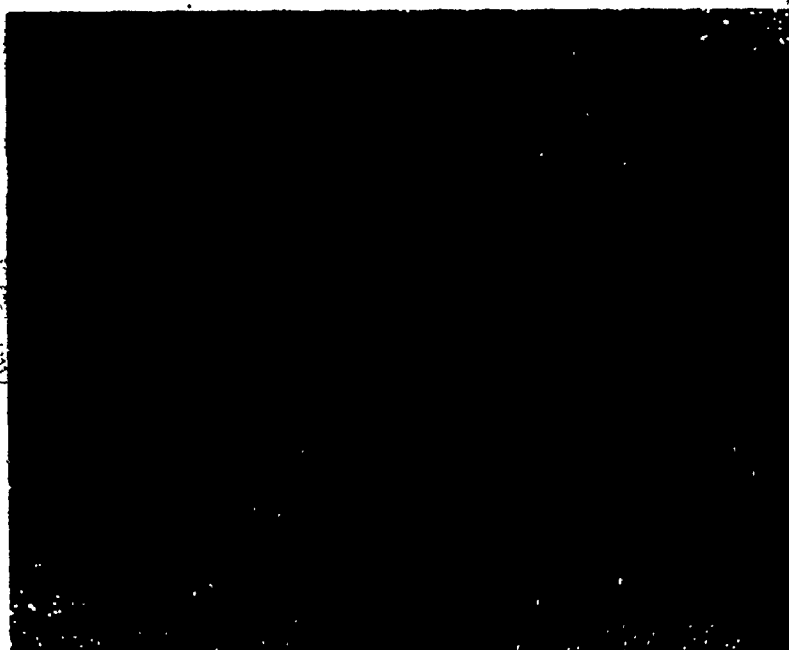


Plate 3.13G Mg distribution

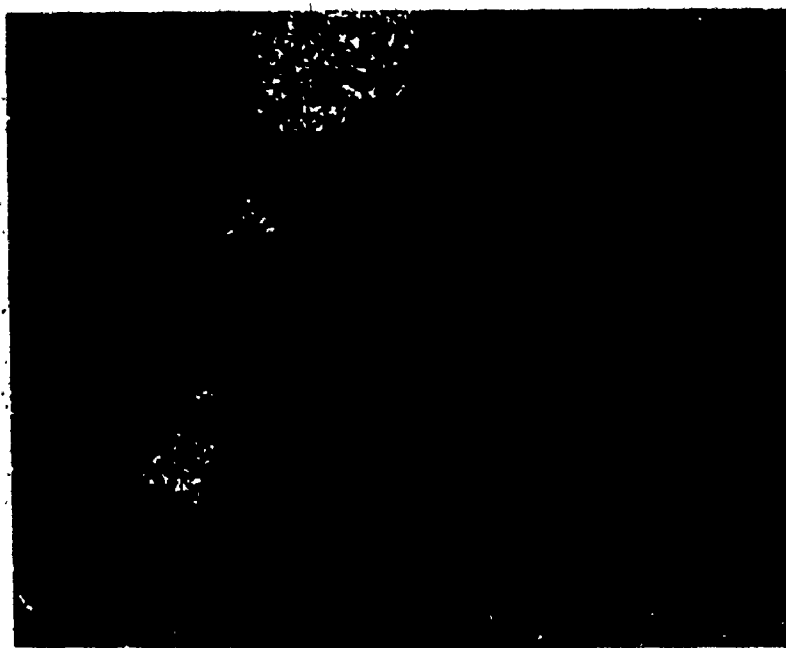


Plate 3.13H P distribution

rock. Plate 3.7A is a photograph of the section of the slide that was analyzed. Repeated X-ray emission scans with the detector windows set to record Si, Al, K, Fe, Mg, Ti and Cr (Plates 3.7B through 3.7H respectively) reveal much of the compositional variation of the rock. The even distribution of the dots representing Si, Al, K, Fe, Mg and Cr indicate a massive fine grained rock consisting of quartz, K-feldspar, chlorite and dolomite with possible some fuchsite. The Ca window was not scanned but the whole rock X-ray diffraction powder scan of this sample (EB-2) shows that dolomite is present but not magnesite. Therefore, the Mg present is in the dolomite and possibly in the chlorite.

The Ti scan (Plate 3.7G), indicates the presence of rutile clusters. Fuchsite does not appear on the XRD whole rock scans and may only be present in less than detectable amounts. The Cr scan indicates no distinct areas of Cr concentration and provides no specific evidence of the presence of Cr-rich mica. The Cr response is probably best interpreted as Cr background levels only.

As has been pointed out previously, dolomite is present, and it is important to note that while both the Mg scan and the Cr scan have resulted in approximately the same numbers of dots per unit area, they are not equivalent.

The information obtained from another portion of the EB-2 slide (Plate 3.8) is almost the only evidence in the entire thesis study that might point to the presence of ankerite in these rocks. This plate is of a twinned portion of a carbonate grain at 2000x magnification. Ca, Fe, and Mg are present. A minor amount of Si

was also present but was not recorded onto a plate. While the number of dots are not an accurate quantitative measure, there is clearly enough Ca to distribute between both Mg and Fe. This grain of carbonate could be made up of an intimate mixture of dolomite and ankerite, but that possible mixture is not represented by the twinning evident in the picture in Plate 3.8A. Plate 3.9 (50x magnification) from sample MG-11 shows a similar distribution of the Ca, Fe and Mg as Plate 3.8C (Sample EB-2) and ankerite may be present.

The only feldspar mentioned by the previous workers as being a part of the quartz-carbonate rock was albite. When a major peak appeared at 27.95° of two theta with copper K alpha radiation, on a large number of the XRD whole rock scans, it was assumed by the present author to be albite. However, data from the SEM scans has shown that the feldspar detected is a potassium feldspar rather than albite. Plate 3.10 (1050x magnification from sample MG-11) is a good example. The greatest concentration of dots from the Si, Al and K scans fall in the same area.

Plate 3.11 (50x magnification, sample MV-2) is an example of a group of large pyrite grains in the fine grained mass of the quartz-carbonate rock. The pyrite grains show evidence of strain by their broken and corroded edges.

Plate 3.12 (50x magnification) is a portion of the slide from sample EB-2 and indicates the unexpected presence of barium. The other minerals in evidence are pyrite, dolomite, magnesite and chlorite. This X-ray emission scan series shown in Plate 3.12 is the only one to show the presence of barium presumably in barite.

Plate 3.13 at 1000x magnification is another portion of the slide from sample EB-2 and is the only indication of a phosphorous bearing mineral (possibly apatite) in the thin sections studied. The other minerals present in the slide include quartz, K-feldspar, dolomite, rutile and pyrite.

Chapter Four Discussion and Conclusions

The quartz-carbonate rocks of the Kirkland Lake-Larder Lake Gold Camp were studied by X-ray diffraction, SEM X-ray emission, and polished thin sections. A few chemical analyses were used to support the quantitative X-ray diffraction data.

The data obtained from the whole rock powder scans and presented in Table 3.1 indicate the frequency of occurrence of the various major mineral components of the rocks. As shown by Table 3.1 quartz, dolomite, magnesite and feldspar make up the bulk of the rock in most cases. All of the rock samples which contained quartz, dolomite and magnesite were analyzed quantitatively with the X-ray diffractometer using copper K alpha radiation and a series of oscillations between 26° and 33° of two theta. The data obtained were plotted within the limits of two percentage error fields that were established by analyzing two series of prepared standards (Section 2.3). The amounts of quartz, dolomite and magnesite present in the quartz-dolomite-magnesite fraction of the rock, i.e. the major bulk of the rock, were then calculated and plotted on triangular graph paper (Figure 3.3). The error margin in this data is variable as reported in Section 3.2, and ranges between 0.31 and 66.0 percent. The mean value for each sample is the one plotted on the triangular graph.

The polished thin sections were examined using transmitted

light and electron microscopy. These techniques revealed the fabric of the rock and to a certain extent, the accessory mineralogy. Due to the high proportion of carbonate minerals present, and the fine grained nature of the rocks, apart from the veins, transmitted light microscopy was of somewhat limited use for mineral identification. It is better used to document the texture and fabric of the rocks. Scanning electron microscopy, using the Stereoscan instrument (SEM) to obtain X-ray emission scans of a polished section of the rock, was most useful in confirming the presence and mapping the distribution of the various minerals known to be present on the basis of XRD. The Stereoscan proved to be of additional use in that it indicated the presence of minerals such as barite, that were quite unexpected. It also revealed that the mineralogical complexity of the quartz-carbonate rocks persists below normal optical resolution (1000x) (Plates 3.7 to 3.13)

Quartz is a major component of most samples of the quartz-carbonate rock across the length of the study area. Massive quartz stockworks are most common in the eastern portion of the study area and are especially prominent in the Kerr-Addison mine. The general pervasiveness of the quartz is not always immediately obvious in hand sample and the thin sections (Section 3.3) show that quartz exists in abundance even in the fine grained main mass of the rock. This abundance of quartz in both the veins and the main rock mass may be indicative of one of three things; 1) the original unaltered rock contained considerably more quartz than is immediately apparent in what appear to be fresh samples, 2) the introduction of quartz,

which apparently accompanied the shearing and brecciation along the Larder Lake Break, was much more penetrative a phenomenon than simple fracture filling, 3) the quartz is entirely metamorphic and was introduced into a carbonated ultramafic. Fluid filled inclusions are common in the larger quartz grains and could perhaps provide an avenue of investigation into the physical conditions prevailing at the time of the quartz vein formation.

Recent chemical analyses of the quartz-carbonate rock (Appendix III) consistently show 10% to 12% Fe_2O_3 , and therefore a point which arose early in the study was whether or not ankerite is indeed present in the rocks, as had been maintained by some of the earlier workers (Section 1.3). This proved to be a question that was very difficult to answer. The ankerite XRD peak pattern was never detected on the whole rock X-ray diffraction scans. There are two possible explanations for this; 1) either ankerite is not present, or 2) it is only present with dolomite, and only in small quantities (relative to dolomite). With copper K alpha radiation the main peak of dolomite is at 30.985° of two theta and the main ankerite peak is at 30.952° , or a lateral difference on the strip chart paper of less than one millimeter with respect to the scan and chart speeds. The secondary peaks confirm that dolomite is present in every case of a peak appearing at 30.95° to 31.00° two theta. The secondary peaks of ankerite are extremely small (Figure 2.1) and would almost certainly not be far enough above the background for a positive identification. Ankerite could indeed be present but totally masked, on the X-ray diffractometer scans, by dolomite. As has been mentioned in

Section 3.4 ankerite may have been detected in the X-ray emission scans. In the two thin sections (Plates 3.8 and 3.9) the dots representing Ca, Mg and Fe occur in the same area of the slide, however this pattern of dots could also be produced by a fine mixture of dolomite and chlorite. The quartz-carbonate rocks often have rust stains, presumably limonite, on the weathered surfaces and from the investigations described in this study, the iron responsible for the rusty weathering may be in ankerite; however both chlorite or pyrite are nearly always significant accessory minerals in the quartz-carbonate rocks and either mineral must be considered as a potential source of iron. Ankerite then is a possible component of the rocks either as a discrete mineral or in solid solution with the dolomite.

The feldspar component of the quartz-carbonate rocks also requires further clarification. As the matter now stands, there is evidence to support the presence of both albite and a potassium feldspar, possibly orthoclase. The evidence in favor of the presence of albite comes from the whole rock X-ray diffraction scans. A major peak appears at 27.91° of 2θ , or a d spacing of 3.196\AA on about twenty of the whole rock scans. The d spacing of the main albite peak is 3.196\AA and the main peak of orthoclase is at 3.18\AA . The presence of albite is confirmed by the secondary peaks or rather the lack of them. The secondary peaks of albite are all rather small but when they do appear above the background level they match the albite pattern. The secondary peaks of orthoclase are both large and numerous and would certainly show if they were present on the whole rock scans. The evidence which supports the presence of orth-

oclase comes from the X-ray emission scans where the dots representing potassium are found in the same areas as those representing silica and aluminum.

The strain and shearing which is evident in the rocks along the Larder Lake Break is also reflected microscopically. The strain patterns visible in every quartz grain are clear evidence of the stresses applied to the rocks both before and after the introduction of the quartz veins. The larger pyrite grains are often broken and show evidence of grinding on the edges. The carbonate minerals have recrystallized and therefore show no evidence of stresses in the form of undulatory extinction. The large complex carbonate grains may in fact be the result of the recrystallization of a few smaller grains into one larger one.

The major purpose of this investigation, as stated in previous sections, was to determine the carbonate mineralogy of the quartz-carbonate rocks. The data presented show that the carbonate fraction of the rocks consists of dolomite and magnesite. The presence of magnesite as such has not been reported previously from the study area and in the author's opinion, this fact alone goes a long way toward settling the controversy over the origin of the quartz-carbonate horizon. Magnesite rich exhalative iron formations are not a notable feature of Archean greenstone belts.

The magnesite is not evenly distributed across the study area but is concentrated into four general areas along the Larder Lake Break; 1) at the western end of the camp between Kenogami Lake and Swastika, 2) in the central part of Gauthier Township, 3) in the

area north and west of the town of Larder Lake, and 4) in the eastern end of the camp between the McGarry-McVittie Township line and the old Chesterfield Mine (now part of the Kerr-Addison Mine).

Magnesite also occurs in other scattered locations across the camp (Map 2). On the other hand dolomite is evenly distributed across the camp and has been detected in virtually every sample.

The second question addressed by this study was the possible proximity of a specific combination of carbonates to the known gold deposits in the camp. As can be seen from Map 2 there is a reasonably good correlation between the known deposits and the occurrence of magnesite along the Larder Lake Break. This correlation is not complete but may be well worth consideration in future gold exploration in the Kirkland Lake-Larder Lake Gold Camp. A case in point is the so called Duffy Option (Map 2 No. 85) south of Kirkland Lake along the Larder Lake Break. Kerr-Addison Mines has conducted extensive exploration in this area, based on the fact that the rocks look identical to those in the Kerr-Addison green carbonate ore bodies. There is only background level gold in the Duffy Option; there is also no magnesite in the Duffy Option rocks, whereas the Kerr-Addison ore bodies contain substantial amounts of magnesite. The reason for this correlation was not pursued in this study but it may be that the presence of magnesite contributes to a geochemical environment which is conducive to the precipitation of gold.

In summary then the carbonate minerals present in the Kirkland Lake-Larder Lake Gold Camp are dolomite, magnesite and possibly ankerite; and, there is some positive correlation between the presence of magnesite and the occurrence of known gold deposits.

APPENDICES

0

Appendix I X-ray Diffractometry

A. X-ray Diffractometers

The machines used for the analysis of the rock powders were standard Philips Norelco vertical powder diffractometers. The sample is placed in the sample container and the diffracted radiation is detected in a scintillation counter housed in an arm which rotates about the sample container. The scan results were recorded with a rate meter and displayed on a horizontal strip chart recorder.

The copper K alpha radiation was produced at 30 kilovolts, and 16 milliamps and was graphite monochromated. The detector arm was set to rotate at one degree per minute. The chart recorder ran at 2 cm per minute and the linear range was established at 10^3 for the whole rock scans and 10^4 or 10^5 for the ratio scans.

C. Aluminum Sample Holders

The dry rock powders were packed into the aluminum sample holders by the following method. The top opening of the sample holder was closed by taping a piece of glass to the holder. The holder was then inverted and the powder placed into the hole and pressed with a small spatula. Care was taken not to tamp down the powder. The powder surface was leveled and another piece of glass taped across the opening. The holder was turned right side up again and the first piece of glass removed to expose a smooth, flat and presumably random powder surface.

Appendix II Source of Minerals for Standard Mixtures

A Quartz

The quartz was from the study area. Milky white clean looking quartz was chosen and crushed using a jaw crusher and disc pulverizer. The resulting chips were ground in the shatter box for five minutes. The quartz powder was placed in a glass vial and warm 10% HCl was added and left overnight to digest any carbonates. The remaining powder was dried and stored for future standard preparations. The XRD trace from the quartz powder matched the accepted standard.

B Dolomite

The dolomite was from the Lockport Formation near Hamilton. The rock was crushed as described above. The XRD trace matched the accepted dolomite JCPDS Standard No. 11-78 to within 0.1A d spacing for all the peaks.

C Magnesite

The magnesite is from St. Stanislaus County, California and is available from Wards Scientific Co. No. 46W4830. The rock was crushed as described above. The XRD trace matched the accepted magnesite standard JCPDS No. 8-479 to within 0.01A d spacing for all the peaks.

Appendix III Chemical Analysis of Quartz-Carbonate Rocks by XRF

The following data was obtained by Mr. L. A. Tihor

Sample No.	Map No.	SiO ₂	Fe ₂ O ₃	MgO	CaO	Na ₂ O	K ₂ O	TiO ₂
KA-9n	50	41.26	10.75	23.87	14.88	2.49	0.07	0.33
MIS-4	84	52.17	9.47	11.67	11.34	0.08	3.93	0.56
LL-3	86	52.98	9.64	20.12	8.10	0.42	2.32	0.28
LL-9	87	45.61	10.91	35.42	2.67	0.62	0.00	0.20
709-9	80	16.52	12.11	21.40	40.77	1.68	0.10	0.31
SWA-6-12	63	42.43	11.81	26.48	12.20	0.02	0.07	0.35
MG-1003	23	33.15	15.78	38.19	4.33	0.49	0.42	0.41
KA-3n	46	33.77	13.04	31.67	13.38	0.91	1.20	0.36
KA-4n	47	44.58	10.55	30.06	9.18	0.00	0.05	0.25
KA-8n	49	36.71	12.73	29.45	8.91	1.62	1.90	0.36

- mineral percentages

BIBLIOGRAPHY

- Bain, G. W., 1933. Wall-Rock Mineralization along Ontario Gold Deposits. Econ. Geol. vol. 28, pp 705-743
- Brock, R. W., 1907. The Larder Lake District. Bureau of Mines, Ontario, No. 4.
- Cook, H. C. 1922. Kenogami, Round and Larder Lake Area, Timiskaming District, Ontario. G.S.C. Memoir 131, No. 112 Geological Series
- Goodwin, A. M., 1965. Mineralized Volcanic Complexes in the Porcupine-Kirkland Lake, Noranda Region, Canada., Econ. Geol. vol. 60, pp 955-971
- Hewitt, D. F., 1963. The Timiskaming Series of the Kirkland Lake Area. Can. Mineral. vol. 7, pp 479-522
- Hutchison, C. S., 1974. Laboratory Handbook of Petrographic Techniques. John Wiley and Sons 527p.
- Hyde, R. pers. comm.
- Jenny, C. P., 1941. Geology of Omega Mine, Larder Lake, Ontario. Econ. Geol. vol. 36 pp 424-447
- Lovell, H. L., 1972. The Geology of the Eby and Otto Area, District of Timiskaming. ODM Geol. Rept. 99.
- MacLean, A., 1965. Geology of Lebel Township. ODM Bull. 150.
- Mehar, J. and Doning, C. Geology of Kerr-Addison Mines Ltd. Mine Handout Sheet
- Moorhouse, W. W., 1959. The Study of Rocks in Thin Section. Harper and Rowe. N. Y.

Ridler, R. H., 1969. The Relationship of Mineralization to Volcanic Stratigraphy, in the Kirkland Lake Area, Ontario.

Unpub. PhD Thesis, U. of Wisconsin.

1970. Relationship of Mineralization to Volcanic Stratigraphy in the Kirkland-Larder Lake Area, Ontario.

Geol. Ass. Can. Proc. vol. 21, pp 33-48

Rogers, A. F. and Kerr, P. F., 1942. Optical Mineralogy. McGraw-Hill. N. Y.

Thompson, J. E., 1943. Geology of McGarry and McVittie Townships, Larder Lake Area. 50th Annual Rept. vol. L, Part vii.

ODM.

1944. Geology of Gauthier Township, East Kirkland Lake Area. 50th Annual Rept. vol. L, Part viii. ODM.

Tully, D. W., 1963. The Geology of the Upper Canada Mine. Geol. Ass. Can. Proc. vol. 15, pp 61-86

Warne, S. St. J., 1962. A Quick Field or Laboratory Staining Scheme for the Differentiation of the Major Carbonate Minerals. J. Sed. Pet. vol. 32, pp 29-33